https://doi.org/10.15407/ufm.24.04.654

An.D. ZOLOTARENKO [1,2,*], Ol.D. ZOLOTARENKO [1,2,], Z.A. MATYSINA [1], N.A. SHVACHKO [1,3], N.Y. AKHANOVA [4,5], M. UALKHANOVA [5], D.V. SCHUR [1,6,***], M.T. GABDULLIN [4], M.T. KARTEL [2], Yu.M. SOLONIN [1,****], Yu.I. ZHIRKO [6], D.V. ISMAILOV [5,7], A.D. ZOLOTARENKO [1], and I.V. ZAGORULKO [8]**

[1] I.M. Frantsevych Institute for Problems of Materials Science of the N.A.S. of Ukraine, Omeljan Pritsak Str., UA-03142 Kyiv, Ukraine
[2] O.O. Chuiko Institute of Surface Chemistry of the N.A.S. of Ukraine, 17 General Naumov Str., UA-03164 Kyiv, Ukraine
[3] Kyiv National University of Construction and Architecture, 31 Povitroflotskyi Ave., UA-03037 Kyiv, Ukraine
[4] Kazakh–British Technical University, 59 Tole bi Str., 050000 Almaty, Kazakhstan
[5] Al-Farabi Kazakh National University, 71 Al-Farabi Ave., 050040 Almaty, Kazakhstan
[6] Institute of Applied Physics of the N.A.S. of Ukraine, 58 Petropavlivska Str., UA-40000 Sumy, Ukraine
[7] NJSC 'K.I. Satbayev Kazakh National Research Technical University', 22a Satbaev Str., 050013 Almaty, Kazakhstan
[8] G.V. Kurdyumov Institute for Metal Physics of the N.A.S. of Ukraine, 36 Academician Vernadsky Blvd., UA-03142 Kyiv, Ukraine

* a.d.zolotarenko@gmail.com, ** o.d.zolotarenko@gmail.com, *** dmitry.schur@gmail.com, **** solonin@ipms.kiev.ua

HYDROGEN IN COMPOUNDS AND ALLOYS WITH *A*15 STRUCTURE

In the present work, a theoretical study of atomic ordering in the A_3BC_x alloy is carried out. The mutual influence of the ordering and solubility of impurity C in the A_3B alloy is studied. The dependences of solubility on the composition of the

Citation: An.D. Zolotarenko, Ol.D. Zolotarenko, Z.A. Matysina, N.A. Shvachko, N.Y. Akhanova, M. Ualkhanova, D.V. Schur, M.T. Gabdullin, M.T. Kartel, Yu.M. Solonin, Yu.I. Zhirko, D.V. Ismailov, A.D. Zolotarenko, and I.V. Zagorulko, Hydrogen in Compounds and Alloys with *A*15 Structure, *Progress in Physics of Metals*, **24**, No. 4: 654–685 (2023)

alloy, temperature, degree of long-range order are found and studied. In addition, the criteria for the manifestation of extremity in the concentration and temperature dependences of solubility are obtained. The atomic ordering is studied using the average-energies' method; the features of the *C* impurity solubility in the A_3B alloy are elucidated using the configuration method. Experiments confirming the results of the theory are currently unknown to authors. However, the available experimental data on determining the temperatures of martensitic transformation (T_m) and superconducting transition (T_c) for the Nb_3SnH_x alloy allow us to hope and assert a possible agreement between the data of theory and experiment.

Keywords: crystal structure, *A*15-type structure, alloys, compounds, metal hydrides, hydrogen, phase transformations, order–disorder transitions, solubility.

1. Introduction

Currently, active research is being carried out on the behaviour of hydrogen (H_2) in compounds and in alloys [1–26] for its storage and for changing the properties of crystal lattices. For hydrogen energy, the scientific field of nanotechnology is very important, as studies show a high level of activation of alloys in nanodispersed powders for hydrogen sorption. Today, the storage and transportation of hydrogen is the main problem of hydrogen energy, for the solution of which not only metals [18–26] and alloys [1–17] are involved, capable of being a working fluid in modern hydrogen storage (HS), but also carbon nanostructures (fullerenes [27–31], fullerites [32, 33], endofullerenes [34–37], and others [38–41]) as promising hydrogen sorbents [42–48]. The role of carbon nanostructures (CNS) in hydrogen energy is due to their variety and to the wide range of methods for their synthesis [49–58]. This makes it possible to create modern composites based on the listed materials using 3*D* printing technologies [59–62].

Compounds and alloys with the *A*15 structure are actively studied in connection with their interesting and unusual properties, such as the transition to the superconducting state, the manifestation of structural instability, Butterman–Barrett martensitic transformations at low and room temperatures, non-vanishing atomic ordering, a decrease of atomic volume to sizes smaller than those of pure components, a strong temperature dependence of the magnetic susceptibility and electrical resistance, an anomalously high heat capacity at room temperature, *etc.* (see, *e.g.*, [64–67]). Many published works confirm the technological purpose of these materials. Typical representatives of these systems are Nb_3Sn, V_3Si, V_3Ga, V_3Ge alloys.

An important role in the formation of alloy properties is played by impurities, which usually include Al and Sb in Nb_3Sn alloys, and Al, Si, Ti in V_3Si, V_3Ga, V_3Ge alloys. In this case, systems of the $A_3B_{1-x}C_x$ type are formed, where ***A*** is Nb or V, ***B*** is Sn, Si, Ga or Ge, and ***C*** is an impurity that partially replaces *B* atoms [68, 69]. The impurity, as a rule,

contributes to a decrease of the temperature T_m of the structural martensitic transformation, and suppresses it at a high concentration x. A subsequent monotonic decrease of the temperature T_c of the transition to the superconducting state is observed.

Of particular interest is the Nb_3SnH_x alloy [70], in which the hydrogen atoms (H) are located not in sites legal for tin atoms, but in alternative positions of niobium atoms. In the presence of hydrogen (H_2), the temperatures T_m, T_c also decrease, and at $x > 0.1$, no structural transformation is observed.

The properties of alloys and compounds A_3B, $A_3B_{1-x}C_x$, A_3BC_x are associated with the features of their crystal structure. Theoretical and experimental studies of the atomic ordering process in the A_3B alloy with the $A15$ structure [71–78] made it possible to reveal its features and reveal the injustice of the usual ideas about ordering and, in particular, about the order–disorder phase transition. The criteria for the manifestation of extremity in the concentration and temperature dependence of solubility can be obtained [79–81].

2. Formulation of the Problem

Consider an alloy A_3B of the structure $A15$ with impurity C. Figure 1 shows the crystal lattice of the A_3BC_x alloy, where $0 < x \le 3$. There are three types of sites, legal respectively for atoms A, B and C. The sites of the first type, located on the faces of cubic cells, form three orthogonal sets of linear chains. Sites of the second type lie at the vertices and centres of cubes. Sites of the third type form three mutually perpendicular sets of linear chains, alternative to the positions of the first-type sites. Sites of the first and second types are completely occupied by atoms A and B, the process of atomic ordering takes place at these sites, they are crystallographically unequal, *i.e.*, they have a different kind of environment by neighbouring sites. C atoms enter the crystal from the external environment, the degree of the third-type sites filling with C atoms is determined by the solubility of component C, and some of the third-type sites are vacant.

We assume that the crystal lattice is geometrically ideal, the type of its structure does not change with temperature and composition changes, and the alloy is single-phase. Correlation in the filling of lattice sites by atoms will not be taken into account. We will take into account the pair interaction of atoms at distances

$$r_1 = \frac{d\sqrt{2}}{4} \approx 0.354d,\ r_2 = \frac{d\sqrt{5}}{4} \approx 0.559d,\ r_3 = \frac{d}{2}, \qquad (1)$$

where d is the crystal lattice constant.

A site of the first type has two neighbouring sites of the first type at a distance of r_3 and four sites of the second type at a distance of r_2.

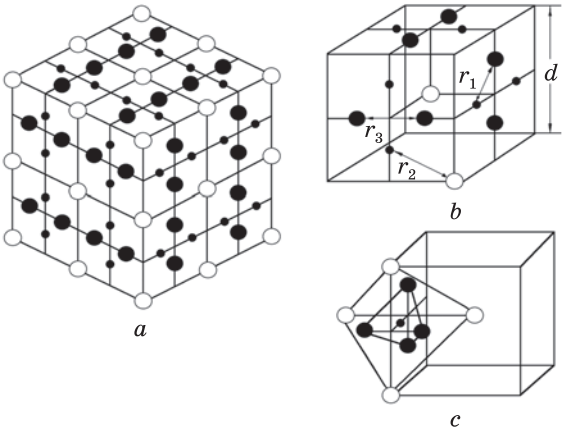

Fig. 1. Crystal lattice of A_3BC_x alloy, where large solid, large open, and small solid circles denote sites of the first, second, and third types, legal for atoms *A*, *B*, and *C*; (*a*) orthogonal sets of linear chains of the first and third type; (*b*) sites of the unit cell of the crystal; (*c*) tetrahedra of sites of the first and second types with the *C* atom in the centre [1]

A site of the second type has 12 neighbouring sites of the first type at a distance of r_2. A site of the third type has four nearest neighbouring sites of the first type at a distance of r_1 and four sites of the second type at a distance of r_2. The site of the third type is located in the centre of two tetrahedra.

Let us introduce into consideration the quantities characterizing the lattice, the composition of the alloy, the distribution of atoms across the lattice sites and the interatomic interaction:

N is the total number of atoms *A*, *B* in the alloy A_3B, the same number of sites of the first and second type;

N_A, N_B, N_C, N_V — the number of atoms, respectively, *A*, *B*, *C* and vacancies *V* (at the sites of the third type) in the alloy A_3BC_x;

$$N^{(1)} = \frac{3N}{4}, \quad N^{(2)} = \frac{N}{4}, \quad N^{(3)} = \frac{3N}{4} \tag{2}$$

— the number of sites of the first, second and third types, respectively; $N_A^{(1)}$, $N_A^{(2)}$, $N_B^{(1)}$, $N_B^{(2)}$, $N_C^{(3)}$ — the numbers of atoms *A*, *B*, *C* at type *i* sites = 1, 2, 3;

$$a = \frac{N_A}{N}, \quad b = \frac{N_B}{N}, \quad c = \frac{N_C}{N^{(3)}}, \quad \upsilon = \frac{N_V}{N^{(3)}} \tag{3}$$

— concentrations of *A*, *B*, *C* atoms and vacancies,

$$a + b = 1,\ 0 \le c \le 1,\ x = 3c. \tag{4}$$

$$\begin{cases} P_A^{(1)} = \dfrac{N_A^{(1)}}{N^{(1)}}, \quad P_B^{(1)} = \dfrac{N_B^{(1)}}{N^{(1)}}, \quad P_C^{(3)} = \dfrac{N_C^{(3)}}{N^{(3)}}, \\ P_A^{(2)} = \dfrac{N_A^{(2)}}{N^{(2)}}, \quad P_B^{(2)} = \dfrac{N_B^{(2)}}{N^{(2)}}, \quad P_V^{(3)} = \dfrac{N_V^{(3)}}{N^{(3)}}, \end{cases} \tag{5}$$

$$\begin{cases} P_A^{(1)} = \dfrac{N_A^{(1)}}{N^{(1)}}, \quad P_B^{(1)} = \dfrac{N_B^{(1)}}{N^{(1)}}, \quad P_C^{(3)} = \dfrac{N_C^{(3)}}{N^{(3)}}, \\ P_A^{(2)} = \dfrac{N_A^{(2)}}{N^{(2)}}, \quad P_B^{(2)} = \dfrac{N_B^{(2)}}{N^{(2)}}, \quad P_V^{(3)} = \dfrac{N_V^{(3)}}{N^{(3)}}, \end{cases} \tag{6}$$

— probabilities of type $i = 1, 2, 3$ filling sites with atoms of grade A, B, C and vacancies V;

$$\eta = 4\,(P_A^{(1)} - a) \tag{7}$$

— the degree of long-range order in the placement of atoms A, B at sites i;

$$\begin{gathered} \upsilon'_{\alpha\beta} = \upsilon_{\alpha\beta}(r_1), \ \upsilon''_{\alpha\beta} = \upsilon_{\alpha\beta}(r_2), \quad \upsilon^*_{\alpha\beta} = \upsilon_{\alpha\beta}(r_3), \\ \upsilon'_{\alpha c} = \upsilon_{\alpha c}(r_1), \ \upsilon''_{\alpha c} = \upsilon_{\alpha c}(r_2), \quad \alpha, \beta = A, B \end{gathered} \tag{8}$$

— energies with the inverse sign of the atoms pair interaction at the distances indicated in parentheses.

To solve the tasks, it is necessary to calculate the free energy of the alloy,

$$F = E - kT \ln W - kTN \ln\lambda, \tag{9}$$

and investigate the conditions of thermodynamic equilibrium of the system. Here, E is the internal configuration energy of the alloy, determined by the energies of interatomic interaction; k is the Boltzmann constant; T is the absolute temperature; W is the thermodynamic probability of the system state, determined by the distribution of atoms across sites in accordance with the rules of combinatorics; λ is the activity of atoms C.

Initially, we will study the process of atomic ordering in the alloy and the effect of impurities on it.

3. Atomic Order in A_3B Alloy with C Impurity

We use the method of average energies, taking into account that the configuration energy E is determined by the sum of the all pairs of atoms interatomic interaction average energies at distances r_1, r_2, r_3. Then the energy E is equal to

$$\begin{aligned} E = &-N_{AA}(r_3)\upsilon^*_{AA} - N_{BB}(r_3)\upsilon^*_{BB} - N_{AB}(r_3)\upsilon^*_{AB} - \\ &- N_{AA}(r_2)\upsilon''_{AA} - N_{BB}(r_2)\upsilon''_{BB} - N_{AB}(r_2)\upsilon''_{AB} - \\ &- N_{AC}(r_1)\upsilon'_{AC} - N_{BC}(r_1)\upsilon'_{BC} - N_{AC}(r_2)\upsilon''_{AC} - N_{BC}(r_2)\upsilon''_{BC}, \end{aligned} \tag{10}$$

where $N_{\alpha\beta}$ are the numbers of α, $\beta = A$, B and C atom pairs at the distances indicated in parentheses. The interaction of C–C pairs in (10) is

not taken into account, since, as a rule, $N_C \ll N^{(3)}$. The numbers of atomic pairs without taking into account correlation can easily be determined through probabilities $P_\alpha^{(i)}$:

$$N_{AA}(r_3) = N^{(1)}P_A^{(1)^2},\ N_{BB}(r_3) = N^{(1)}P_B^{(1)^2},\ N_{AB}(r_3) = 2N^{(1)}P_A^{(1)}P_B^{(1)},$$

$$N_{AA}(r_2) = 12N^{(2)}P_A^{(1)}P_A^{(2)},\ N_{BB}(r_2) = 12N^{(2)}P_B^{(1)}P_B^{(2)},$$

$$N_{AA}(r_3) = N^{(1)}P_A^{(1)^2},\ N_{BB}(r_3) = N^{(1)}P_B^{(1)^2},\ N_{AB}(r_3) = 2N^{(1)}P_A^{(1)}P_B^{(1)},$$

$$N_{AC}(r_1) = 4N^{(3)}P_A^{(1)}P_C^{(3)},\ N_{BC}(r_1) = 4N^{(3)}P_B^{(1)}P_C^{(3)},$$

$$N_{AC}(r_2) = 4N^{(3)}P_A^{(2)}P_C^{(3)},\ N_{BC}(r_2) = 4N^{(3)}P_B^{(2)}P_C^{(3)}. \qquad (11)$$

The thermodynamic probability W according to the rules of combinatorics is

$$W = \frac{N^{(1)}!}{N_A^{(1)}!N_B^{(1)}!}\cdot\frac{N^{(2)}!}{N_A^{(2)}!N_B^{(2)}!}\cdot\frac{N^{(3)}!}{N_C^{(3)}!N_\upsilon^{(3)}!}, \qquad (12)$$

where numbers $N_\alpha^{(i)}$ can also be expressed, according to (5), in terms of probabilities $P_\alpha^{(i)}$.

The calculation of the free energy F (9), expressed taking into account the ratios (5), (11) in terms of probabilities $P_\alpha^{(i)}$, leads to the result

$$F = -N^{(1)}(P_A^{(1)^2}\upsilon_{AA}^* + P_B^{(1)^2}\upsilon_{BB}^* + 2P_A^{(1)}P_B^{(1)}\upsilon_{AB}^*) -$$

$$-12N^{(2)}\left[P_A^{(1)}P_A^{(2)}\upsilon_{AA}'' + P_B^{(1)}P_B^{(2)}\upsilon_{BB}'' + (P_A^{(1)}P_B^{(2)} + P_A^{(2)}P_B^{(1)})\upsilon_{AB}''\right] -$$

$$- 4N^{(3)}P_C^{(3)}(P_A^{(1)}\upsilon_{AC}' + P_B^{(1)}\upsilon_{BC}' + P_A^{(2)}\upsilon_{AC}'' + P_B^{(2)}\upsilon_{BC}'') +$$

$$+ kT\left[N^{(1)}(P_A^{(1)}\ln P_A^{(1)} + P_B^{(1)}\ln P_B^{(1)}) + N^{(2)}(P_A^{(2)}\ln P_A^{(2)} + P_B^{(2)}\ln P_B^{(2)}) +\right.$$

$$\left. + N^{(3)}(P_u^{(3)}\ln P^{(3)} + P_\upsilon^{(3)}\ln P_\upsilon^{(3)})\right] - kTN^{(3)}P^{(3)}\ln\lambda. \qquad (13)$$

Taking into account the ratios (6), we find the free energy F depending on the composition of the alloy, the degree of long-range order and temperature:

$$F = -\frac{3}{4}N\left\{a^2(\upsilon_{AA}^* + 4\upsilon_{AA}'') + b^2(\upsilon_{BB}^* + 4\upsilon_{BB}'') + 2ab(\upsilon_{AB}^* + 4\upsilon_{AB}'') +\right.$$

$$+\frac{1}{2}\eta\left[a(4w'' - w^*) - \upsilon_{BB}^* + \upsilon_{AB}^* + 4(\upsilon_{BB}'' - \upsilon_{AB}'')\right] +$$

$$+ 4c\left[a(\upsilon_{AC}' + \upsilon_{AC}'') + b(\upsilon_{BC}' + \upsilon_{BC}'')\right] +$$

$$\left. + c\eta\left[\upsilon_{AC}' - \upsilon_{BC}' - 3(\upsilon_{AC}'' - \upsilon_{BC}'')\right] + \frac{1}{16}\eta^2(12w'' - w^*)\right\} +$$

$$+\frac{3}{4}kTN\left[\left(a+\frac{1}{4}\eta\right)\ln\left(a+\frac{1}{4}\eta\right)+\left(b-\frac{1}{4}\eta\right)\ln\left(b-\frac{1}{4}\eta\right)+\right.$$

$$+\frac{1}{3}\left(a-\frac{3}{4}\eta\right)\ln\left(a-\frac{3}{4}\eta\right)+\frac{1}{3}\left(b-\frac{3}{4}\eta\right)\ln\left(b-\frac{3}{4}\eta\right)+$$

$$+c\ln c+(1-c)\ln(1-c)-\frac{3}{4}kTNc\ln\lambda. \qquad (14)$$

where

$$w^{*}=2\upsilon^{*}_{AB}-\upsilon^{*}_{AA}-\upsilon^{*}_{BB},\quad w''=2\upsilon''_{AB}-\upsilon''_{AA}-\upsilon''_{BB}. \qquad (15)$$

The minimum free energy condition $\frac{\partial F}{\partial\eta}=0$ gives the equation

$$kT\ln\frac{\left(a+\frac{1}{4}\eta\right)\left(b+\frac{3}{4}\eta\right)}{\left(a-\frac{3}{4}\eta\right)\left(b-\frac{1}{4}\eta\right)}=R_1\eta+R_2+R_3c, \qquad (16)$$

determining the equilibrium value of the long-range order degree depending on the temperature and composition of the alloy. In (16),

$$R_1=6w''-\frac{1}{2}w^{*},$$

$$R_2=2a\left(4w''-w^{*}\right)-2\left(\upsilon^{*}_{BB}-\upsilon^{*}_{BB}\right)+8\left(\upsilon''_{BB}-\upsilon''_{AB}\right),$$

$$R_3=4\left(\upsilon'_{AC}-\upsilon'_{BC}\right)-12\left(\upsilon''_{AC}-\upsilon''_{BC}\right). \qquad (17)$$

Equation (16) differs from the equilibrium equations of the ordering alloys theory at equivalent sites by the presence of terms R_2, R_3c, which do not have a multiplier of the long-range order degree. The presence of these terms determines the features of the η dependence on the temperature and concentration of impurity C.

To illustrate the features of the $\eta=\eta(T,c)$ dependence such graphs were constructed for an alloy of stoichiometric composition for components A, B, *i.e.*, for $a=3/4$, $b=1/4$. In this case, equation (16) takes the form

$$kT\ln\frac{\left(1+\frac{1}{3}\eta\right)(1+3\eta)}{(1-\eta)^2}=R_1\eta+R_2+R_3c. \qquad (18)$$

Figure 2 shows graphs of the long-range order parameter (η) temperature dependence, constructed according to the formula (18) for energy parameters equal to

$$R_1=0.72,\ R_2=0.005,\ R_3=\pm1\ [\text{eV}], \qquad (19)$$

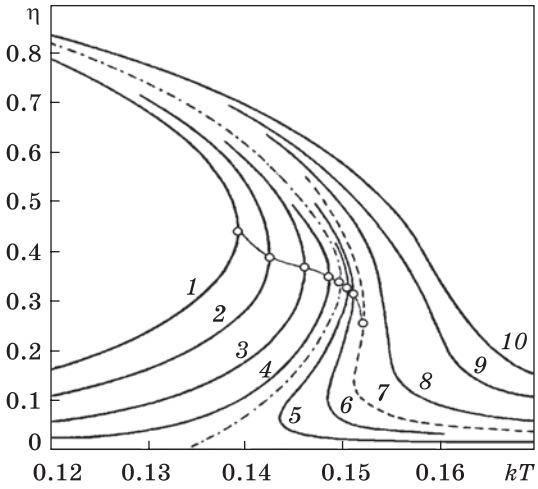

Fig. 2. Temperature dependence of the long-range order parameter according Eq. (18) [1] for $R_1 = 0.72$ eV, $R_2 = 0.005$ eV, $R_3 = -1$ eV (curves *1–6*), $R_3 = 1$ eV (curves *8–10*) and the impurity C concentration for curves *1–10*, equal to (*1*) 0.025, (*2*) 0.017, (*3*) 0.01, (*4*) 0.006, (*5*) 0.004, (*6*) 0.002, (*7*) 0, (*8*) 0.003, (*9*) 0.009, (*10*) 0.013. For the dashed curve, $R_2 = R_3 = 0$. Extreme points are marked with open circles

and different concentrations of impurity C. The extreme points are marked with circles on these graphs, allowing us to estimate the possible temperature of the phase transition, which is somewhat smaller in magnitude than the temperature of the extreme point. To compare and identify the features of the dependence $\eta = \eta(T, c)$, Fig. 2 shows a graph corresponding to the energy parameters $R_1 = 0.72$ eV, $R_2 = 0$, $R_3 = 0$ (dashed curve). The graphs $\eta(T)$, passing to the left of the dashed curve correspond to the case when $R_2 + R_3 c < 0$, and to the right — to the case when $R_2 + R_3 c > 0$. The dotted line shows the curve for alloy A_3B at $c = 0$.

As can be seen in Fig. 2, for all curves *1–10* constructed at $R_2 + R_3 c \neq 0$, the long-range order degree does not vanish at any temperatures. This means that the ordered state of the alloy is equilibrium at all temperatures. In the presence of an extremum on the curve $\eta(T)$, an order-order phase transition is possible in the A_3BC_X alloy. In the absence of an extremum, the long-range order parameter monotonically decreases with increasing temperature (curves *8–10*).

The studies carried out in [77, 78] showed that the upper branch of curves *1–4* (when $R_2 + R_3 c < 0$) to the extreme point corresponds to stable (deep minimum of free energy) and metastable (less deep minimum of free energy) states, and the lower branch of these curves corresponds to an unstable state (maximum of free energy). Therefore, the order-order phase transition without changing the sign of the long-range order degree should not occur in these cases.

The order–order phase transition without changing the grade of sites is possible at $R_2 + R_3 c > 0$, *i.e.*, for states described by curves *5–7* with an extreme point for which $R_3 < 0$. For such curves, with an increase of the c concentration, the temperature of the extreme point, and consequently, the order–order transition temperature decreases, and when,

at sufficiently large concentrations of c, it turns out that $R_2 + R_3 c > 0$, the order–order phase transition disappears.

In [70], the transition temperatures to the superconducting state and the martensitic transformation temperatures in the Nb_3SnH_x system were determined depending on the hydrogen concentration. With an increase of the hydrogen concentration, the temperatures of these transformations decreased, and at $x > 0.1$ ($c > 0.03$) there was no martensitic transformation, *i.e.*, the transition of the cubic phase to the tetragonal phase disappeared. If we take into account that the degree of long-range order can be characterized by the degree of tetragonality

$$\eta \propto \left| \frac{d}{c} - 1 \right|, \tag{20}$$

(d and c are the parameters of the tetragonal lattice) as it was done, for example, in [82], it can be assumed that the experimental data [70] indirectly correspond to the results of our calculations, and it is hoped that direct experiments to identify the effect of the impurity concentration C on the ordering temperature of the A_3BC_x alloy with the $A15$ structure will confirm the results our theoretical calculations.

Minimizing the free energy (14) by the concentration of c, *i.e.*, the condition $\partial F/\partial \eta = 0$ allows you to determine the solubility of the impurity C. The calculation gives the formula

$$c = \left(1 + \frac{1}{\lambda} \exp \frac{-Q - \frac{1}{4} R_3 \eta}{kT} \right)^1, \tag{21}$$

where

$$Q = Q(a) = 4\left[a(\upsilon'_{AC} + \upsilon''_{AC}) + b(\upsilon'_{BC} + \upsilon''_{BC}) \right], \tag{22}$$

determines the equilibrium concentration of impurity C in the A_3BC_x alloy as a function of composition, order parameters and temperature.

At low solubility, when $c \ll 1$, formula (21) is simplified as

$$c = \lambda \exp \frac{Q(a) + \frac{1}{4} R_3 \eta}{kT}. \tag{23}$$

For a disordered alloy, when $\eta = 0$, formula (23) takes the form

$$c_0 = \lambda \exp \frac{4a(\upsilon'_{AC} + \upsilon''_{AC}) + 4b(\upsilon'_{BC} + \upsilon''_{BC})}{kT}. \tag{24}$$

According to the latter formula, the concentration dependence of the impurity C solubility in an unordered alloy is monotonic. With a change in the concentration of a, the solubility of c changes from

$$c_A = \lambda \exp \frac{4(\upsilon'_{AC} + \upsilon''_{AC})}{kT} \text{ when } a = 1$$

(solubility of impurity C in pure component A) up to

$$c_B = \lambda \exp \frac{4(\upsilon'_{BC} + \upsilon''_{BC})}{kT} \text{ when } a = 0$$

(solubility of impurity C in pure component B).

The temperature dependence of solubility is also monotonic and depends on the sign of the magnitude Q (22), *i.e.*, on the signs of the energies $\upsilon'_{\alpha\beta}$, $\upsilon''_{\alpha\beta}$. At $Q > 0$, the solubility of c decreases with increasing temperature, at $Q < 0$ it increases.

The atomic order determines both the increase and decrease of the component C solubility depending on the sign of the value R_3 (see (17)), *i.e.*, on the ratios between the energies $\upsilon'_{\alpha\beta}$, $\upsilon''_{\alpha\beta}$.

At $\eta \neq 0$, the solubility of component C is determined by the formula

$$c = c_0 \exp \frac{R_3 \eta}{kT}. \qquad (25)$$

At $R_3 < 0$, the solubility of component C in the ordered alloy decreases due to the atomic order in comparison with the solubility in the disordered alloy; if $R_3 > 0$, then, on the contrary, the atomic order increases the solubility.

The solubility of component C in A_3B alloy can be studied using the configuration method, which is more consistent and can reveal features in the configuration and temperature dependence of solubility, in particular, to determine the possibility of extreme manifestations of these dependencies.

4. Solubility of Impurity C in A_3B Alloy

We calculate the free energy of the alloy using the method of configurations, *i.e.*, taking into account the possibility of forming different configurations of atoms A, B around each atom C. It is necessary to determine the free energy term, depending on the concentration of c and containing the energies of the pair interaction of atoms AC, BC.

The configuration of atoms A, B in sites of the first and second types around a site of the third type is characterized by indices lj, where the number l determines the number of atoms A in sites of the first type, and the number j determines the number of atoms A in sites of the second type.

The energy of the atom C in the site of the third type with the lj-th configuration is equal to

$$\upsilon_{lj} = l\alpha' + (4-1)\beta' + j\alpha'' + (4-j)\beta'', \qquad (26)$$

where

$$\alpha' = \upsilon_{AC}(r_1) = \upsilon'_{AC},$$

$$\beta' = \upsilon_{BC}(r_1) = \upsilon'_{BC},$$

$$\alpha'' = \upsilon_{AC}(r_2) = \upsilon''_{AC},$$

$$\beta'' = \upsilon_{BC}(r_2) = \upsilon''_{BC}. \quad (27)$$

The number of the third-type sites with the lj-th configuration occupied by C atoms is denoted by N_{lj}, and the number of all such sites with the lj-th configuration $-Q_{lj}$. The latter can easily be expressed in terms of probabilities $P_{\alpha}^{(i)}$:

$$Q_{lj} = N^{(3)} \frac{4!}{l!(4-l)!} P_A^{(1)l} P_B^{(1)(4-l)} \frac{4!}{j!(4-l)!} P_A^{(2)j} P_B^{(2)(4-j)}. \quad (28)$$

The configuration internal energy and thermodynamic probability can be written as

$$E = -\sum_{l,j=0}^{4} N_{lj}\upsilon_{lj}\ , \quad (29)$$

$$W = \sum_{l,j=0}^{4} \frac{Q_{lj}!}{N_{lj}!(Q_{lj}-N_{lj})!}. \quad (30)$$

The free energy (9) will be equal to

$$F = -\sum_{l,j=0}^{4} N_{lj}\upsilon_{lj} - kT\sum_{l,j=0}^{4}\left[Q_{lj}\ln Q_{lj} - N_{lj}\ln N_{lj} - (Q_{lj}-N_{lj})\ln(Q_{lj}-N_{lj})\right]. \quad (31)$$

The expression (31) does not contain a term containing the activity of C atoms, since it is convenient to minimize the free energy by the method of an indefinite Lagrange multiplier, which is proportional to the activity.

We compose the function $F + \nu\varphi$, where

$$\phi \equiv \sum_{l,j=0}^{4} N_{lj} - N_C = 0 \quad (32)$$

is a condition for the connection of numbers N_{ij}.

The equilibrium conditions of the system are written as

$$\frac{\partial F}{\partial N_{lj}} + \nu\frac{\partial\phi}{\partial N_{lj}} = 0\,, \quad (33)$$

where ν is the Lagrange multiplier matched to the coupling condition (32).

Substituting the free energy F (31) and the function φ (32) in Eq. (33), we find the equilibrium equations

$$-\upsilon_{lj} + kT\left[\ln N_{lj} - \ln(Q_{lj}-N_{lj})\right] + \nu = 0, \quad l,j = 0,\ 1,\ 2,\ 3,\ 4, \quad (34)$$

from which we determine the numbers N_{lj} of C atoms in the sites of the third type with the lj-th configuration:

$$N_{lj} = Q_{lj}\left(\frac{1}{D}\exp\frac{-\upsilon_{lj}}{kT} + 1\right)^{-1}, \tag{35}$$

where

$$D = \exp\frac{-\nu}{kT}. \tag{36}$$

For relatively small numbers of the third type sites filling with atoms C, when $c \ll 1$, the formulas (35) are simplified and can be written as

$$N_{lj} = DQ_{lj}\exp\frac{\upsilon_{lj}}{kT},\ l,\ j = 0,\ 1,\ 2,\ 3,\ 4. \tag{37}$$

Summing these numbers over all possible configurations, according to (32) we find the equilibrium concentration of C atoms in the alloy

$$c = \frac{N_C}{N^{(3)}} = \frac{1}{N^{(3)}}\sum_{l,j=0}^{4} N_{lj} = DK_1^4K_2^4, \tag{38}$$

where

$$K_1 = P_A^{(1)}\exp\frac{\alpha'}{kT} + P_A^{(1)}\exp\frac{\beta'}{kT},\ K_2 = P_A^{(2)}\exp\frac{\alpha''}{kT} + P_B^{(2)}\exp\frac{\beta''}{kT}. \tag{39}$$

The obtained formulas (38), (39) together with the ratios (6) determine the solubility of component C in alloy A_3B depending on the alloy composition, temperature, degree of long-range order and energy parameters.

In the case of an unordered alloy, when $\eta = 0$, the solubility of the impurity C is determined by the formula

$$c_0 = D\left(a\exp\frac{\alpha'}{kT} + b\exp\frac{\beta'}{kT}\right)^4\left(a\exp\frac{\alpha''}{kT} + b\exp\frac{\beta''}{kT}\right)^4. \tag{40}$$

5. Concentration Dependence of the Impurity Solubility in Disordered Alloy

Let us find out the concentration dependence of the impurity C solubility in disordered alloy A_3B.

We investigate the function (40), more precisely the function

$$f(a) = \sqrt[4]{\frac{c_O}{D}} = \left(a\exp\frac{\alpha'}{kT} + b\exp\frac{b'}{kT}\right)\left(a\exp\frac{\alpha''}{kT} + b\exp\frac{b''}{kT}\right), \tag{41}$$

on the extremum. Equality $\partial f/\partial a = 0$ defines the necessary condition for the extremity of this function. After calculations, this condition can be written in the form

$$\exp\frac{\alpha'}{kT} - \exp\frac{\beta'}{kT} = -G\left(\exp\frac{\alpha''}{kT} - \exp\frac{\beta''}{kT}\right), \tag{42}$$

where

$$G = \left(a \exp \frac{\alpha'}{kT} + b \exp \frac{\beta'}{kT} \right) \Big/ \left(a \exp \frac{\alpha''}{kT} + b \exp \frac{\beta''}{kT} \right) > 0 , \qquad (43)$$

and concentrations a, b correspond to the extremum point, *i.e.*, $a = a_e$, $b = 1 - a_e$.

Eq. (42) can be fulfilled if, when the interatomic distance r changes from r_1 to r_2, the difference $\exp(\alpha/kT) - \exp(\beta/kT)$ changes sign, *i.e.*, if $\exp(\alpha'/kT) - \exp(\beta'/kT) > 0$ we have $(\alpha''/kT) - \exp(\beta''/kT) < 0$ or *vice versa*.

From (42) and (43), the concentration of a_e can be determined, at which the function $f = f(a)$ is extreme. The calculation gives the formula

$$a_e = \frac{\exp \dfrac{\beta'}{kT}}{\exp \dfrac{\alpha'}{kT} - \exp \dfrac{\beta'}{kT}} - \frac{\exp \dfrac{\beta''}{kT}}{\exp \dfrac{\alpha''}{kT} - \exp \dfrac{\beta''}{kT}} . \qquad (44)$$

The extremum of the function $f(a)$ will occur if the a_e value calculated by this formula falls within the interval $0 \le a_e \le 1$. If it turns out that $a_e < 0$ or $a_e > 1$, then in the interval $0 \le a \le 1$, the function $f(a)$ will be monotonic.

The calculation of the second derivative $\partial^2 f/\partial a^2$ gives the result

$$\frac{\partial^2 f}{\partial a^2} = 2 \left(\exp \frac{\alpha'}{kT} - \exp \frac{\beta'}{kT} \right) \left(\exp \frac{\alpha''}{kT} - \exp \frac{\beta''}{kT} \right). \qquad (45)$$

In the latter relation, if there is an extremum, the expressions in parentheses have different signs. This means that $\partial^2 f/\partial a^2$ and the solubility of $c_0 = c_0(a)$ at point $a = a_e$ has a maximum.

The latter circumstance means that, under the condition of a change in the sign of the difference $\exp(\alpha/kT) - \exp(\beta/kT)$ as a result of the interatomic distance $r_1 \to r_2$ change, the solubility of impurity C in a disordered alloy A_3B with a composition near $a = a_e$ will be higher than the solubility of this impurity in pure components A and B.

Figure 3 shows graphs of the concentration dependence of the solubility of $c_0 = c_0(a)$, more precisely, the functions $f = f(a)$ (41), constructed for a certain temperature and various values of energy parameters α', β', α'', β'', such that $\exp(\alpha'/kT) - \exp(\beta'/kT) > 0$ (Fig. 3, *a*) and $\exp(\alpha'/kT) - \exp(\beta'/kT) > 0$ (Fig. 3, *b*).

For Fig. 3, *a*, the energy parameters for a certain temperature and a_e concentration (44) of extreme points on curves *1–5* are equal to

$$\begin{gathered} \exp(\alpha'/kT) = 9,\ \exp(\alpha''/kT) = 1, \\ \exp(\beta'/kT) = 1,\ \exp(\beta''/kT) = 1.5,\ 2,\ 3,\ 4,\ 5, \\ a_e = 1.4375\ (1)\ \text{(no maximum)},\ 0.9375\ (2), \\ 0.6875\ (3),\ 0.6042\ (4),\ 0.5625\ (5). \end{gathered} \qquad (46)$$

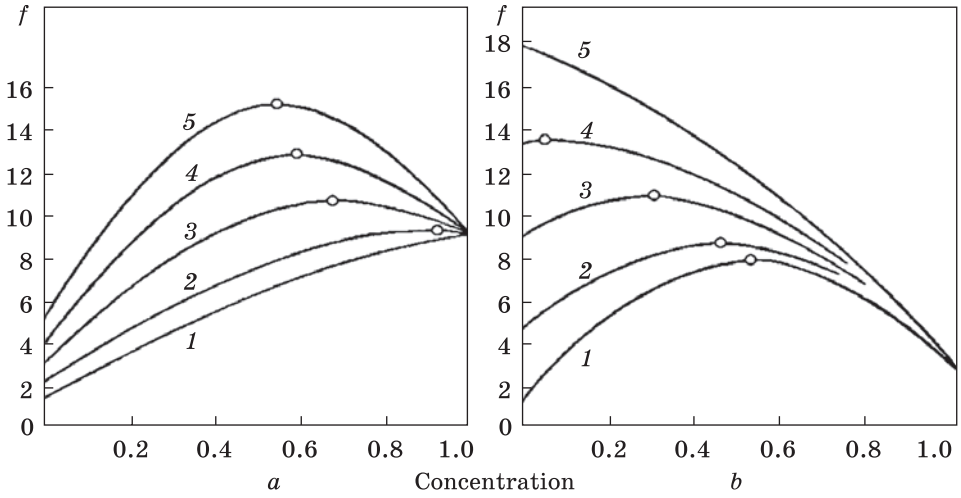

Fig. 3. Solubility of *C*-impurity *vs*. concentration in disordered A_3B alloy [1]: (*a*) $\exp(\alpha'/(kT)) = 9$, $\exp(\alpha''/(kT)) = 1$, $\exp(\beta'/(kT)) = 1$, $\exp(\beta'/(kT)) = 9$, $\exp(\beta''/(kT)) = 1.5, 2, 3, 4, 5$ (curves *1–5*); (*b*) $\exp(\alpha'/(kT)) = 1$, $\exp(\alpha''/(kT)) = 3$, $\exp(\beta'/(kT)) = 9$, $\exp(\beta''/(kT)) = 1.125, 0.5, 1, 1.5, 2$ (curves *1–5*). Extreme points are marked with circles on the curves

For Fig. 3 (*b*), they are equal to

$$\begin{gathered}\exp(\alpha'/kT) = 1,\ \exp(\alpha''/kT) = 3,\\ \exp(\beta'/kT) = 9,\ \exp(\beta''/kT) = 0.125,\ 0.5,\ 1,\ 1.5,\ 2,\\ a_e = 0.5408\ (1),\ 0.4625\ (2),\ 0.3125\ (3),\\ 0.0625\ (4),\ -0.4375\ (5)\ \text{(no maximum)}.\end{gathered} \tag{47}$$

In accordance with the selected values of the energy parameters, all curves *1–5* in Fig. 3 at $a = 1$ converge at one point with an ordinate equal to

$$f_A = \exp\frac{\alpha'}{kT}\exp\frac{\alpha''}{kT},\ \textit{i.e.},\ c_A = D\exp\frac{4\alpha'}{kT}\exp\frac{4\alpha''}{kT}, \tag{48}$$

determining the solubility of impurity *C* in the pure component *A*.

For $a = 0$, the function f_b, which determines the solubility of the impurity *C* in the pure component *B*, is equal to

$$f_B = \exp\frac{\beta'}{kT}\exp\frac{\beta''}{kT},\ \textit{i.e.},\ c_B = D\exp\frac{4\beta'}{kT}\exp\frac{4\beta''}{kT}, \tag{49}$$

and it is different for curves *1–5* in Fig. 3.

With an increase of the energy parameter β'' in accordance with the formulas (40) or (41), (48), (49) the solubility of the impurity in the alloy increases, and since all curves *1–5* have the same ordinate at $a = 1$, the concentration of the extreme point a_e shifts to the region of large concentrations of *a*.

Knowledge of the $c_0 = c_0(a)$ experimental dependence can allow us to estimate the energy parameters $\alpha = \alpha'$, α'', $\beta = \beta'$, β'' using the obtained formula (40) and to obtain information about the change of the atoms pair interaction energies with a change of the interatomic distance $r(r_1 \to r_2)$, which is a scientific interest.

If the energy parameters of the alloy are known from independent experiments, *e.g.*, for systems A–C, B–C, using the obtained formula (40), it is possible to determine the concentration dependence of the impurity C solubility in the disordered alloy A–B structure $A15$, and, in particular, by the formula (44) to predict the possibility of an extreme dependence of $c_0(a)$.

6. Temperature Dependence of the Impurity Solubility in Disordered Alloy

Consider the temperature dependence of the function $f = f(T)$ (41). Let us first find out the possibility of the function $f = f(T)$ extremum manifestation. The condition $\partial f/\partial T = 0$ gives the equation

$$a\alpha' \exp\frac{\alpha'}{kT} + b\beta' \exp\frac{\beta'}{kT} = -G\left(a\alpha'' \exp\frac{\alpha''}{kT} + b\beta'' \exp\frac{\beta''}{kT}\right), \qquad (50)$$

where the value $G > 0$ is determined by the formula (43).

First of all, we note that the condition (50) of the extreme temperature dependence of the impurity C solubility in A_3B alloy with structure $A15$ differs from those obtained earlier for other structures [82–104].

Equality (50), taking into account that $G > 0$ can be fulfilled if the dependences of the atoms pair interaction energies on the interatomic distance $\alpha = \alpha(r)$, $\beta = \beta(r)$ are such that when the distance r changes from the value r_1 to the value r_2, their sign (or one of them) changes to the opposite.

As an illustration, Fig. 4 shows graphs of the solubility temperature dependence, constructed for energy parameters α', β', α'', β'' such that the energies of α', α'' are chosen of different signs, and the energies of β', β'' are both of the same and different signs. The graphs in Fig. 4 were constructed for concentrations $a = b = 0.5$, *i.e.*, for the function f, defined by the expression

$$4f = 4f(T) = \left(\exp\frac{\alpha'}{kT} + \exp\frac{\beta'}{kT}\right)\left(\exp\frac{\alpha''}{kT} + \exp\frac{\beta''}{kT}\right), \qquad (51)$$

and energy parameters α', β', α'', β'' are equal as follow [eV]:

$$\alpha' = -0.012;\ \beta' = -0.036;\ \alpha'' = 0.026;$$

$$\beta'' = -0.032;\ -0.012;\ 0;\ 0.012;\ 0.02;\ 0.03. \qquad (52)$$

As can be seen in Fig. 4, the temperature dependence of the impurity C solubility in disordered alloy A_3B (curves *1–4*) is extreme, while

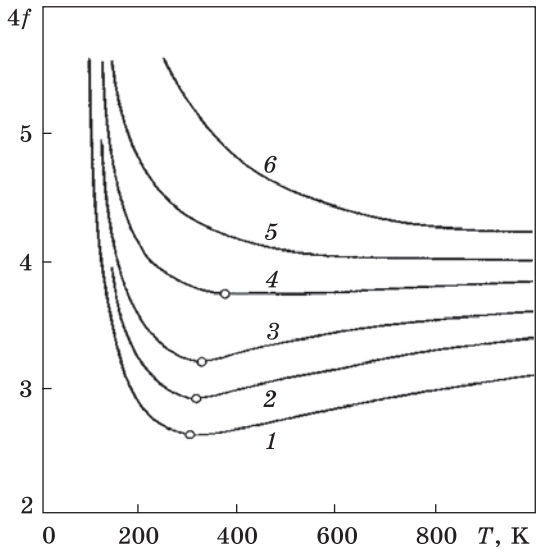

Fig. 4. Solubility of the *C* impurity *vs*. temperature in disordered alloy A_3B composition, $a = b = 0.5$ [1]. Graphs are plotted for the following energy parameters (eV): $\alpha' = -0.012$; $\alpha'' = 0.026$; $\beta' = -0.036$; $\beta'' = -0.032$; -0.012; 0; 0.012; 0.02; 0.03 (curves *1*–*6*). Circles on the curves indicate the positions of the minima

the energies β' and β'' have different signs only for the 4-th curve. In all these cases, with an increase of temperature from zero, the solubility of component *C* first drops sharply, reaching a minimum, and then gradually increases. At the same time, with an increase of β'' energy, both the solubility and the temperature T_0, corresponding to the minimum, increase; the latter for curves *1*–*4* is equal to

$$(1)\ 310,\ (2)\ 320;\ (3)\ 360;\ (4)\ 375\ [\mathrm{K}]. \qquad (53)$$

In case of curves *5*, *6* realization, temperature dependence of the impurity *C* solubility is monotonous, though at the same time and energy α', α'' and β', β'' change sign, *i.e.*, the condition of changing the sign of the energies $\alpha(r)$, $\beta(r)$ (or one of them) when the interatomic distance r changes from r_1 to r_2 for the extremum of the *C* component solubility temperature dependence is necessary, but not sufficient.

Thus, with a change of the disordered alloy A_3B with the structure *A*15 temperature, the solubility of the impurity *C* can both increase and decrease. Note that the presence of a minimum in the dependence $c_0 = c_0(T)$ can be used (by annealing at a temperature of T_0) to reduce the solubility of component *C* in alloy A_3B in order to change its physical properties in the right direction. Knowledge of the energy parameters from independent experiments (*e.g.*, on the solubility of impurity *C* in pure components *A* and *B*) can allow using the obtained formula (40) and equation (50) to determine the temperature dependence of component *C* in the alloy under consideration and, in particular, to reveal the possible extremity of this dependence.

7. Atomic Order Effect on the Impurity Solubility

The effect of the long-range degree on the solubility of impurity C in alloy A_3B is convenient to find out for the relative solubility of $s = c/c_0$. Taking into account the formulas (38)–(40) and (6), the relative solubility of s can be represented as

$$s = (1 + \chi_1)^4(1 - 3\chi_2)^4, \tag{54}$$

where

$$\chi_1 = \frac{1}{4}\eta\frac{\exp\dfrac{\alpha'}{kT} - \exp\dfrac{\beta'}{kT}}{a\exp\dfrac{\alpha'}{kT} + b\exp\dfrac{\beta'}{kT}}; \quad \chi_2 = \frac{1}{4}\eta\frac{\exp\dfrac{\alpha''}{kT} - \exp\dfrac{\beta''}{kT}}{a\exp\dfrac{\alpha''}{kT} + b\exp\dfrac{\beta''}{kT}}. \tag{55}$$

The values χ_1, χ_2, proportional to the long-range order parameter η can characterize the degree of the alloy ordering. Their sign and numerical values are determined by the ratio between the energy parameters α', α'' and β', β''. It is easy to verify that the maximum possible values χ_1 and χ_2, are estimated by ratios

$$-1 \le \chi_1 \le \frac{1}{3}, \quad -1 \le \chi_2 \le \frac{1}{3}. \tag{56}$$

Equation (54) represents a surface in three-dimensional space (s, χ_1, χ_2) and determines the relative solubility of impurity C in an ordered alloy A_3B depending on the values of parameters χ_1, χ_2. Fig. 5, *a* shows the appearance of this surface in the range of the parameters χ_1, χ_2 possible values (56). Curved lines on the surface indicate levels of the equal solubility; a number at the curve marks the solubility value of each level. The dotted line with $s = 1$ corresponds to a disordered alloy when $c = c_0$, *i.e.*, when the atomic order does not affect the change of solubility. For levels above this curve, atomic ordering increases the solubility of impurity *C*, and below decreases it.

Fig. 5, *b* shows the levels of equal solubility in the projection onto the plane (χ_1, χ_2) in the region (56) of the parameters χ_1, χ_2 values. All levels of equal solubility and their projections onto the plane (χ_1, χ_2) turn out to be symmetric with respect to the plane perpendicular to the plane (χ_1, χ_2), whose projection onto the plane (χ_1, χ_2) is determined by the equation

$$\chi_1 + \chi_2 = -2/3. \tag{57}$$

Along this straight line, the relative solubility is given by the equation

$$s^{\frac{1}{4}} = 3(1 + \chi_1)^2. \tag{58}$$

From equations (57), (58) we obtain

$$\chi_1 = -1 + 1/\sqrt{3} \approx -0.423, \ \chi_2 \approx -0.244 \ \text{for} \ s = 1. \tag{59}$$

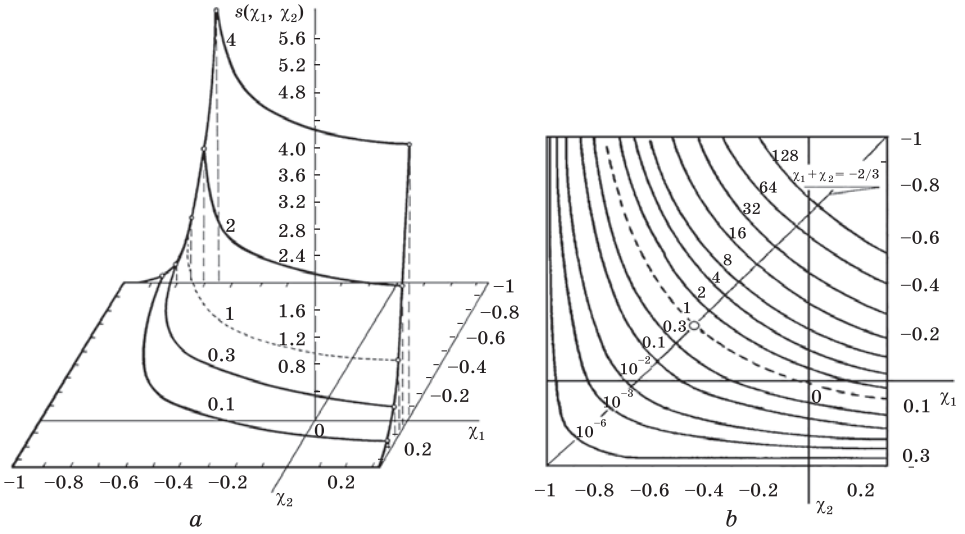

Fig. 5. (*a*) Dependence of the impurity *C* relative solubility on the order parameters (values χ_1 and χ_2) in the A_3B alloy — surface $s(\chi_1,\chi_2)$ [1]. Lines on the surface indicate the levels of equal solubility (numbers in curves). (*b*) The levels of equal solubility in the projection on the plane (χ_1, χ_2) in the range of possible values (56) of the parameters χ_1 and χ_2. A straight line is the projection of the plane of symmetry for the equal solubility levels. A circle marks a point on the line $\chi_1 + \chi_2 = -2/3$ with $s = 1$, which coordinates are equal to $\chi_1 = -0.423$ and $\chi_2 = -0.244$

Therefore, along the straight line (57),

$$\text{at } \chi_1 > -0.423, \text{ we have } s > 1,$$
$$\text{at } \chi_1 < -0.423, \text{ we have } s < 1. \qquad (60)$$

The straight lines $\chi_1 = -1$ and $\chi_2 = 1/3$ on the plane χ_1, χ_2) are also the levels of equal solubility and determine the zero solubility of the *C* component in the A_3B alloy. If we move along the straight line (57) from the point with coordinates $\chi_1 = -1$ and $\chi_2 = 1/3$, then the relative solubility *s* will increase smoothly monotonously approximately to the level $s = 0.3$. Further change of the values χ_1 and χ_2 along the straight line (57) leads to a sharp increase solubility *s*.

Thus, depending on the atomic order and the values of the parameters χ_1 and χ_2, the solubility of the impurity *C* in the A_3B alloy can both decrease and increase. Knowing of the each specific alloy energy parameters from independent experiments can allow us to estimate the parameters χ_1 and χ_2 (55) for any composition and then, according to the formula (54), to determine the effect of atomic ordering on the solubility of impurity *C* in an alloy with structure *A*15. In this case, the degree of the long-range order (η) can be estimated by the formula (16).

It should be noted that with a change of temperature in the alloy, a phase transformation of the first kind with an abrupt change of the long-range order degree $\eta_1 \rightarrow \eta_2$ is possible. In this case, there will be an abrupt change of the parameters χ_1 and χ_2 and the relative solubility of *s*. The latter circumstance will indicate the fact of phase transformation at this temperature in the alloy under study.

8. Discussion

Relevance. A_3B alloys of structure *A*15 have a crystal lattice consisting of two elements, for example, Ti_3Ir consists of titanium and iridium. Each *A* atom is surrounded by six *B* atoms, and each *B* atom is surrounded by six *A* atoms. This structure is also called 'cactus' because of its cactus-like shape [105].

Hydrogen is an important element in *A*15-A_3B alloy because it can significantly affect its physical and mechanical properties. For example, adding hydrogen to *A*15 alloy can improve its elasticity and strength, reduce the coefficient of friction, and provide better corrosion resistance.

In addition, the solubility of hydrogen in *A*15 alloy, such as Nb_3Sn [70, 106], V_3Si [106, 107], Ti_3Al [107, 109], V_3Ga [110], Ti_3Ir [105, 107, 110], Pd_3Ag [111] and others, can vary depending on the conditions to control its properties [68, 69]. For example, depending on the temperature and hydrogen concentration, different levels of strength and hardness of the alloy can be achieved [105].

Therefore, hydrogen is an important element of *A*15 alloy, which can provide improvements in its physical and mechanical properties and provide more precise control over its performance. This makes *A*15 alloys potentially useful in the automotive and aerospace industries.

Type *A*15 hydrogenated intermetallic materials emphasize that they are a special class of compounds consisting of metallic elements such as niobium (Nb) [70], vanadium (V) [90], titanium (Ti) [105, 107–109, 110, 112–115,], chromium (Cr), aluminium (Al) [109], palladium (Pd) [111] and others [68, 69], as well as hydrogen [1–84, 105–115]. These compounds have high structural stability and interesting physical properties, making them important for a variety of applications. Research by scientists has established that the presence of hydrogen does not change the structure of the original *A*15 crystals [110].

One of the main features of *A*15 type hydrogenated intermetallic compounds is their ability to store large quantities of hydrogen. They can absorb hydrogen to high concentrations [110], making them potentially useful as hydrogen storage materials. Research in the proposed work confirms the importance of *A*15 alloys in hydrogen energy, as accumulating and storing hydrogen elements. And they can also be used as catalysts in electrolysis reactions [111], fuel cells and other electro-

chemical systems, which makes them an interesting object in the field of electrochemical activity research.

In general, *A*15-type hydrogenated intermetallic compounds represent an interesting class of alloys with unique physical, mechanical, and electrochemical properties. They have the potential to expand applications in various fields of science, technology and hydrogen energy.

Elements that can be added to the *A*15 alloy to change its properties include [68, 69] magnesium (Mg) [107, 113, 114], silicon (Si) [106, 107], zirconium (Zr) [107, 112, 116], gallium (Ga) [110], iridium (Ir) [105, 110] , tin (Sn) [106, 107], copper (Cu) [107, 116], aluminium (Al) [107, 109], yttrium (Y) [107], palladium (Pd) [107, 106, 117], molybdenum (Mo) [107, 115], silver (Ag) [111]. The addition of magnesium improves the strength and heat resistance of the alloy [107, 113, 114], and silicon and zirconium improve its corrosion resistance [106, 107, 112, 116]. However, when adding these elements, it is necessary to take into account their influence on the properties of the alloy as a whole. Hydrogen, when introduced into the alloy, passes from the surface unit of the hexagonal close-packed areas (h.c.p.) to the subgrid area and, finally, to the suboct area, with the exception of surfaces alloyed with Mo and pure Ti, by way of from the surface face-centred cubic lattice (f.c.c.) area directly to suboct areas [107, 108, 115]. Among these dopants, Mo promotes the diffusion of hydrogen in the surface plane, and Pd most significantly promotes the hydrogen permeation process [107, 108, 115].

When choosing the *A*15 alloy with the largest range of use in industry, you can stop at the aluminium alloy, which contains approximately 4.5% copper.

An interesting fact is that deuterium (^{2}H) in the Ti_3Ir compound occupies interatomic positions in the *A*15 crystal lattice. It forms octahedral complexes with six atoms of titanium (Ti) and iridium (Ir), which are at the vertices and centres of the faces of the corresponding octahedron. Deuterium in this compound has high mobility and is diffuse [105]. In addition, they interact with electrons and other atoms in the crystal lattice, which can affect the physical properties of the compound [105]. However, impurities of other elements can affect the location of deuterium in the crystal lattice. For example, other studies have shown that impurity elements such as oxygen (O) or carbon (C) can replace titanium (Ti) atoms in the crystal lattice and affect the arrangement of deuterium [105].

The analysis of hydrogen solubility in *A*15 crystals has been the subject of many studies in the scientific literature [1–84, 105–118]. Research shows that the solubility of hydrogen depends on many factors, such as temperature, pressure, hydrogen concentration and others.

Regarding the effect of temperature on the solubility of hydrogen in the *A*15 alloy, it is significant. Usually, including alloy V_3Ga, with an

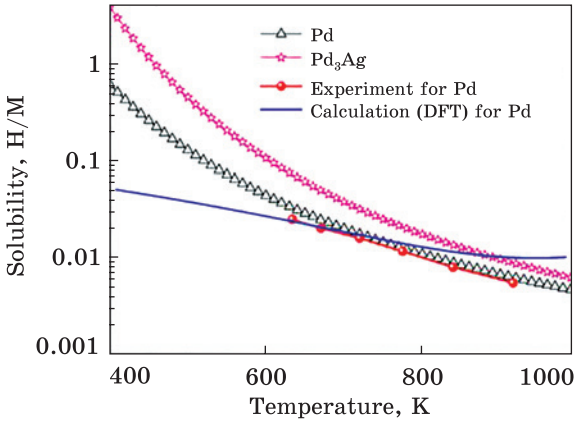

Fig. 6. Data on the solubility of hydrogen in the Pd and Pd_3Ag phases, as well as comparative values obtained in experiments and calculations for pure Pd [111]

increase in temperature, the solubility of hydrogen increases, and a decrease in temperature leads to a decrease in solubility [110]. It is also known that for some *A*15 crystals of the A_3B alloy, for example Pd_3Ag, the solubility of hydrogen increases with decreasing temperature and increasing pressure (Fig. 6) [111]. This is due to a change in the activation energy of the hydrogen dissolution process in the alloy when the temperature changes. It is also worth noting that the solubility of hydrogen in the *A*15 alloy may depend on the concentration of other elements in the alloy, for example, the solubility of hydrogen in the Pd_3Ag alloy depends on the concentration of silver (Ag) in the alloy [111].

*A*15 crystals of the Pd_3Ag alloy are a promising material for hydrogen storage due to their ability to absorb and desorb hydrogen at room temperature (Fig. 6) and pressure [111]. Studies have shown that Pd–Ag alloys have a high hydrogen capacity and the ability to repeatedly cycle hydrogen absorption/desorption. Moreover, Pd–Ag alloys have an advantage over other materials for hydrogen storage due to their stability and resistance to oxidation and interaction with gaseous hydrogen impurities [111].

According to scientific research, the solubility of hydrogen in the *A*15 alloy is quite high and can reach 1 hydrogen atom per 10 metal atoms at low temperatures. The solubility of hydrogen in *A*15 alloy depends on temperature and pressure. For example: the solubility of hydrogen in Nb_3Sn at room temperature and normal pressure, the solubility of hydrogen in such an *A*15 alloy is low (about 0.1 atom per 100 metal atoms) [68, 69, 70, 106].

Considering the solubility of hydrogen in V_3Ga and Ti_3Ir alloys, it can be stated that it is low, since in the V_3Ga alloy at low temperatures the solubility is about 0.1 atomic percent, and at high temperatures it can reach 0.5 atomic percent [110].

For the Ti_3Ir alloy, the solubility at low temperatures is about 0.2 atomic percent, and at high temperatures it can reach 0.8 atomic percent [110].

Research also shows that the solubility of hydrogen can significantly increase under certain conditions. For example, when the pressure or temperature is increased, the solubility can increase to significant values, as can be seen from the alloys V_3Ga [110] and Ti_3Ir [105, 110]. Factors that can affect the solubility of hydrogen in alloys with the *A*15 structure, and in particular Pd_3Ag, V_3Ga, and Ti_3Ir alloys, can be noted: hydrogen pressure, temperature, material composition, and structural composition of the alloy [110, 111]. For example, when hydrogen pressure increases, its solubility in the material also increases [110]. It was also shown that the addition of other elements to the crystal could affect its solubility in hydrogen. That is, the composition of the material and its structure also affect the solubility of hydrogen [110]. Studying these factors can help optimize conditions for efficient hydrogen storage and use in various applications.

Of course, there are also problems when using *A*15 crystals of the A_3B alloy for hydrogen storage, namely the high price of effective sorption alloys (Pd_3Ag) or the problem of hydrogen diffusion through the material, which can lead to hydrogen loss and reduced storage efficiency. Each of these problems has its own solutions, which makes it possible to look at the *A*15 crystals of the A_3B alloy with perspective as promising materials for hydrogen storage in the future [111].

Therefore, the solubility of hydrogen in *A*15-type crystals is a difficult scientific task, which depends on many factors. Despite this, research continues to understand better this process and possible applications of *A*15 type crystals.

An equally important application of the *A*15 alloy is aluminium alloys that contain copper (Cu) as the main alloying element. It has high strength and corrosion resistance, as well as good weldability [107, 109]. The main applications of the *A*15 alloy include the production of aircraft and space structures, as well as in the production of marine ships and other vehicles where high strength and corrosion resistance are required [107, 109, 115]. In addition, the *A*15 alloy can be used in the production of sports equipment, for example, bicycles and golf clubs.

Alloys based on Ti_3Ir are characterized by a high melting point, high hardness and strength. The Ti_3Ir alloy has superconductivity at low temperatures and is used as a material for manufacturing magnets operating in strong magnetic fields. In addition, the Ti_3Ir alloy also has high resistance to oxidation and corrosion due to its high chemical inertness [105], all of which makes it a promising material for use in the production of blades, tools and other products that are subject to high mechanical loads.

The obtained results of this article can be used to study the influence of dissolved hydrogen on the properties of A_3B type alloys with the $A15$ structure and to create new materials with improved characteristics. In addition, these results can be used to study the interaction of hydrogen with other alloys and materials. Overall, this paper opens up many opportunities for further research in the field of hydrogen solubility in alloys with the $A15$ structure. Such research results can be useful for various industries, including energy, the automotive industry, and others where hydrogen storage and use are required.

9. Conclusions

A theoretical study of atomic ordering in A_3B binary alloys of the $A15$ structure with an admixture of the third component C was carried out.

The free energy of the system was calculated depending on the composition of the alloy, temperature, atomic order parameter and energy constants of pairwise interatomic interaction;

An equilibrium equation is found that determines the degree of long-range order as a function of alloy composition and temperature.

The features of the process of atomic ordering for alloys of the structure under consideration have been elucidated;

As established, the first-order phase transition of the order–order type with a jump-like change in the long-range order parameter is possible in the system. A criterion for such a transition has been established.

It is substantiated that with an increase in the concentration of the third component C, the phase transformation temperature should decrease, and at a certain impurity concentration C, the phase transition may disappear. This circumstance indirectly corresponds to the experimental data on the study of phase transformation temperatures in the Nb_3SnH_x system.

The solubility of impurity C in the A_3B alloy was calculated. The calculation was performed both by the average energy method and by the more consistent configuration method.

The dependence of the solubility of component C in the alloy on the concentrations of components A, B, temperature (T) and degree of long-range order (η) was determined.

It has been established that the concentration and temperature dependences of solubility can be extreme: the dependence of solubility on the composition of the alloy may have a maximum; the temperature dependence of solubility may have a minimum.

Criteria for extreme dependence of impurity solubility on alloy composition and temperature were obtained, which turned out to be different from those for alloys of other structures.

The dependence of solubility on the degree of long-range order turned out to be monotonic.

The limits of change of the parameters characterizing the atomic order, at which the atomic ordering increases and decreases the solubility of the *C* component, are established. The phase transformation of the order–order type should cause an abrupt change in the solubility of the *C* impurity.

Graphs of the dependence of the long-range order parameter on temperature for different concentrations of impurity *C* were plotted.

Graphs of the temperature and concentration dependences of the solubility of impurity *C* in the disordered A_3B alloy were plotted for various values of the energy parameters;

Graphs of dependence of relative solubility on parameters characterizing the atomic order have been plotted;

The obtained formulas in the work allow predicting regularities in changes in the degree of long-range order and solubility of impurity *C* in an A_3B alloy of the *A*15 structure with a change in temperature and composition of the alloy;

Formulas obtained for the mutual influence of atomic ordering processes and impurity solubility for each specific alloy, for which the energy parameters characterizing the interatomic interaction are known from independent experiments (*e.g.*, by studying the solubility of impurity *C* in pure components *A* and *B*).

Experiments on the study of the regularities of the solubility of the third component *C* in the A_3B alloy are still known. However, for alloys of other structures, there are experimental works, in which both monotonic (hydrogen in PdPt, FeV, PdNi, oxygen in AgAu) and extreme (carbon in FeNi, hydrogen in FeV) concentration and temperature impurity solubility dependences, as well as a jump in solubility at the ordering temperature (hydrogen in NiFe). Therefore, we can hope that the performance of appropriate experiments for alloys of the *A*15 structure will reveal a correspondence between theory and experiment.

Acknowledgement. The partial support from the National Research Foundation of Ukraine within the project No. 2020.02/0301 'Development of new functional materials for the needs of hydrogen energy' is acknowledged.

REFERENCES

1. Z.A. Matysina, An.D. Zolotarenko, Al.D. Zolotarenko, N.A. Gavrylyuk, A. Veziroglu, T.N. Veziroglu, A.P. Pomytkin, D.V. Schur, and M.T. Gabdullin, *Features of the Interaction of Hydrogen with Metals, Alloys and Compounds. Hydrogen Atoms in Crystalline Solids* (KIM Publishing House: Kyiv: 2022); http://www.aheu.com.ua/Hydrogen.html

2. D.V. Schur, M.T. Gabdullin, V.A. Bogolepov, A. Veziroglu, S.Y. Zaginaichenko, A.F. Savenko,and K.A. Meleshevich, *Int. J. Hydrogen Energy*, **41**, No. 3: 1811 (2016); https://doi.org/10.1016/j.ijhydene.2015.10.011
3. Z.A. Matysina, O.S. Pogorelova, and S.Yu. Zaginaichenko, *J. Phy. Chem. Solids*, **56**, No. 1: 9 (1995); https://doi.org/10.1016/0022-3697(94)00106-5
4. Z.A. Matysina and S.Yu. Zaginaichenko, *Int. J. Hydrogen Energy*, **21**, Nos. 11–12: 1085 (1996); https://doi.org/10.1016/S0360-3199(96)00050-X
5. S.Yu. Zaginaichenko, Z.A. Matysina, I. Smityukh, and V.K. Pishuk, *J. Alloys Compd.*, **330–332**: 70 (2002); https://doi.org/10.1016/S0925-8388(01)01661-9
6. Z.A. Matysina and S.Y. Zaginaichenko, *Rus. Phys. J.*, **59**, No.2: 177 (2016); https://doi.org/10.1007/s11182-016-0757-0
7. S.Y. Zaginaichenko, D.A. Zaritskii, Z.A. Matysina, T.N. Veziroglu, and L.I. Kopylova, *Int. J. Hydrogen Energy*, **40**, No. 24: 7644 (2015); https://doi.org/10.1016/j.ijhydene.2015.01.089
8. Z.A. Matysina and S.Y. Zaginaichenko, *Phys. Met. Metallogr.*, **114**, No. 4: 308 (2013); https://doi.org/10.1134/S0031918X13010079
9. Z.A. Matysina, N.A. Gavrylyuk, M. Kartel, A. Veziroglu, T.N. Veziroglu, A.P. Pomytkin, D.V. Schur, T.S. Ramazanov, M.T. Gabdullin, A.D. Zolotarenko, A.D. Zolotarenko, and N.A. Shvachko, *Int. J. Hydrogen Energy*, **46**, No. 50: 25520 (2021); https://doi.org/0.1016/j.ijhydene.2021.05.069
10. D.V. Shchur, S.Y. Zaginaichenko, A. Veziroglu, T.N. Veziroglu, N.A. Gavrylyuk, A.D. Zolotarenko, M.T. Gabdullin, T.S. Ramazanov, A.D. Zolotarenko, and A.D. Zolotarenko, *Rus. Phys. J.*, **64**, No. 1: 89 (2021); https://doi.org/10.1007/s11182-021-02304-7
11. S.Yu. Zaginaichenko, Z.A. Matysina, D.V. Schur, and A.D. Zolotarenko, *Int. J. Hydrogen Energy*, **37**, No. 9: 7565 (2012); https://doi.org/10.1016/j.ijhydene.2012.01.006
12. Z.A. Matysina, S.Y. Zaginaichenko, D.V. Schur, T.N. Veziroglu, A. Veziroglu, M.T. Gabdullin, Al.D. Zolotarenko, and An.D. Zolotarenko, *Int. J. Hydrogen Energy*, **43**, No. 33: 16092 (2018); https://doi.org/10.1016/j.ijhydene.2018.06.168
13. Z.A. Matysina, S.Y. Zaginaichenko, D.V. Schur, A.D. Zolotarenko, A.D. Zolotarenko, M.T. Gabdulin, L.I. Kopylova, and T.I. Shaposhnikova, *Rus. Phys. J.*, **61**, No. 12: 2244 (2019); https://doi.org/10.1007/s11182-019-01662-7
14. D.V. Schur, A. Veziroglu, S.Yu Zaginaychenko, Z.A. Matysina, T.N. Veziroglu, M.T. Gabdullin, T.S. Ramazanov, An.D. Zolonarenko, and Al.D. Zolonarenko, *Int. J. Hydrogen Energy*, **44**, No. 45: 24810 (2019); https://doi.org/10.1016/j.ijhydene.2019.07.205
15. Z.A. Matysina, S.Yu. Zaginaichenko, D.V. Schur, Al.D. Zolotarenko, An.D. Zolotarenko, and M.T. Gabdulin, *Rus. Phys. J.*, **61**, No. 2: 253 (2018); https://doi.org/10.1007/s11182-018-1395-5
16. Z.A. Matysinaa, An.D. Zolotarenko, Al.D. Zolotarenko, M.T. Kartel, A. Veziroglu, T.N. Veziroglu, N.A. Gavrylyuk, D.V. Schur, M.T. Gabdullin, N.E. Akhanova, T.S. Ramazanov, M. Ualkhanova, and N.A. Shvachko, *Int. J. Hydrogen Energy*, **48**, No. 6: 2271; https://doi.org/10.1016/j.ijhydene.2022.09.225

17. Z.A. Matysina, An.D. Zolotarenko, Ol.D. Zolotarenko, T.V. Myronenko, D.V. Schur, E.P. Rudakova, M.V. Chymbai, A.D. Zolotarenko, I.V. Zagorulko, and O.O. Havryliuk, *Chem., Phys. Technol. Surf.*, **14**, No. 2: 210 (2023); https://doi.org/10.15407/hftp14.02.210
18. Z.A. Matysina and D.V. Shchur, *Rus. Phys. J.*, **44**, No. 11: 1237 (2001); https://doi.org/10.1023/A:1015318110874
19. V.I. Trefilov, D.V. Shchur, V.K. Pishuk, S.Yu. Zaginaichenko, A.V. Choba, and N.R. Nagornaya, *Renewable Energy*, **16**, Nos. 1–4: 757 (1999); https://doi.org/10.1016/S0960-1481(98)00273-0
20. Yu.M. Lytvynenko and D.V. Shchur, *Renewable Energy*, **16**, No. 1–4: 753 (1999); https://doi.org/10.1016/S0960-1481(98)00272-9
21. D.V. Schur, A.A. Lyashenko, V.M. Adejev, V.B. Voitovich, and S.Yu. Zaginaichenko, *Int. J. Hydrogen Energy*, **20**, No. 5: 405 (1995); https://doi.org/10.1016/0360-3199(94)00077-D
22. D.V. Schur, V.A. Lavrenko, V.M. Adejev, and I.E. Kirjakova, *Int. J. Hydrogen Energy*, **19**, No. 3: 265 (1994); https://doi.org/10.1016/0360-3199(94)90096-5
23. S.Y. Zaginaichenko, Z.A. Matysina, D.V. Schur, L.O. Teslenko, A. Veziroglu, *Int. J. Hydrogen Energy*, **36**, No. 1: 1152 (2011); https://doi.org/10.1016/j.ijhydene.2010.06.088
24. S.A. Tikhotskii, I.V. Fokin, and D.V. Schur, *Phys. Solid Earth*, **47**, No. 4: 327 (2011); https://doi.org/10.1134/S1069351311030062
25. A.D. Zolotarenko, A.D. Zolotarenko, A. Veziroglu, T.N. Veziroglu, N.A. Shvachko, A.P. Pomytkin, D.V. Schur, N.A. Gavrylyuk, T.S. Ramazanov, N.Y. Akhanova, and M.T. Gabdullin, *Int. J. Hydrogen Energy*, **47**, No. 11: 7310 (2022); https://doi.org/10.1016/j.ijhydene.2021.03.065xx
26. An.D. Zolotarenko, Al.D. Zolotarenko, A. Veziroglu, T.N. Veziroglu, N.A. Shvachko, A.P. Pomytkin, N.A. Gavrylyuk, D.V. Schur, T.S. Ramazanov, and M.T. Gabdullin, *Int. J. Hydrogen Energy*, **47**, No. 11: 7281 (2021); https://doi.org/10.1016/j.ijhydene.2021.03.025
27. D.V. Schur, S.Y. Zaginaichenko, E.A. Lysenko, T.N. Golovchenko, and N.F. Javadov, *NATO Science for Peace and Security Series C: Environmental Security*: 53 (Springer Science + Business Media B.V: 2008); https://doi.org/10.1007/978-1-4020-8898-8_5
28. D.V. Schur, S.Y. Zaginaichenko, A.D. Zolotarenko, and T.N. Veziroglu, *NATO Science for Peace and Security Series C: Environmental Security*: 85 (Springer Science + Business Media B.V: 2008); https://doi.org/10.1007/978-1-4020-8898-8_7
29. O.D. Zolotarenko, O.P. Rudakova, M.T. Kartel, H.O. Kaleniuk, A.D. Zolotarenko, D.V. Schur, and Y.O. Tarasenko, *Surface*, **12**, No. 27: 263 (2020); https://doi.org/10.15407/Surface.2020.12.263
30. Ol.D. Zolotarenko, O.P. Rudakova, N.E. Akhanova, An.D. Zolotarenko, D.V. Shchur, Z.A. Matysina, M.T. Gabdullin, M. Ualkhanova, N.A. Gavrilyuk, O.D. Zolotarenko, M.V. Chymbai, and I.V. Zagorulko, *Nanosistemi, Nanomateriali, Nanotehnologii*, **20**, No. 3: 725 (2022); https://doi.org/10.15407/nnn.20.03.725
31. D.S. Kerimbekov, N.E. Akhanova, M.T. Gabdullin, Kh.A. Abdullin, D.G. Batryshev, A.D. Zolotarenko, N.A. Gavrylyuk, O,D. Zolotarenko, and D.V. Shchur, *J. Problems in the Evolution of Open Systems*, **24**, Nos. 3–4: 79 (2023); https://doi.org/10.26577/JPEOS.2022.v24.i2.i6

32. V.M. Gun'ko, V.V. Turov, V.I. Zarko, G.P. Prykhod'ko, T.V. Krupska, A.P. Golovan, J. Skubiszewska-Zięba, B. Charmas, and M.T. Kartel, *Chem. Phys.*, **459**: 172 (2015); https://doi.org/10.1016/j.chemphys.2015.08.016
33. M.M. Nishchenko, S.P. Likhtorovich, A.G. Dubovoy, and T.A. Rashevskaya, *Carbon*, **41**, No. 7: 1381 (2003); https://doi.org/10.1016/S0008-6223(03)00065-4
34. N.Y. Akhanova, D.V. Schur, N.A. Gavrylyuk, M.T. Gabdullin, N.S. Anikina, An.D. Zolotarenko, O.Ya. Krivushchenko, Ol.D. Zolotarenko, B.M. Gorelov, E. Erlanuli, and D.G. Batrishev, *Chem., Phys. Technol. Surf.*, **11**, No. 3: 429 (2020); https://doi.org/10.15407/hftp11.03.429
35. Z.A. Matysina, Ol.D. Zolotarenko, O.P. Rudakova, N.Y. Akhanova, A.P. Pomytkin, An.D. Zolotarenko, D.V. Shchur, M.T. Gabdullin, M. Ualkhanova, N.A. Gavrylyuk, A.D. Zolotarenko, M.V. Chymbai, and I.V. Zagorulko, *Prog. Phys. Met.*, **23**, No. 3: 510 (2022); https://doi.org/10.15407/ufm.23.03.510
36. N.Ye. Akhanova, D.V. Shchur, A.P. Pomytkin, Al.D. Zolotarenko, An.D. Zolotarenko, N.A. Gavrylyuk, M. Ualkhanova, W. Bo, and D. Ang, *J. Nanosci. Nanotechnol.*, **21**: 2435 (2021); https://doi.org/10.1166/jnn.2021.18970
37. O.D. Zolotarenko, E.P. Rudakova, A.D. Zolotarenko, N.Y. Akhanova, M.N. Ualkhanova, D.V. Shchur, M.T. Gabdullin, N.A. Gavrylyuk, T.V. Myronenko, A.D. Zolotarenko, M.V. Chymbai, I.V. Zagorulko, Yu.O. Tarasenko, and O.O. Havryliuk, *Chem. Phys. Technol. Surf.*, **13**, No. 3: 259 (2022); https://doi.org/10.15407/hftp13.03.259
38. D.V. Schur, A.D. Zolotarenko, A.D. Zolotarenko, O.P. Zolotarenko, and M.V. Chimbai, *Phys. Sci. Technol.*, **6**, Nos. 1–2: 46 (2019); https://doi.org/10.26577/phst-2019-1-p9
39. M. Baibarac, I. Baltog, S. Frunza, A. Magrez, D. Schur, and S.Y. Zaginaichenko, *Diamond and Related Materials*, **32**: 72 (2013); https://doi.org/10.1016/j.diamond.2012.12.006
40. Al.D. Zolotarenko, An.D. Zolotarenko, V.A. Lavrenko, S.Yu. Zaginaichenko, N.A. Shvachko, O.V. Milto, V.B. Molodkin, A.E. Perekos, V.M. Nadutov, and Yu.A. Tarasenko, *Carbon Nanomaterials in Clean Energy Hydrogen Systems-II*, (Springer, Dordrecht: 2011) p. 127; https://doi.org/10.1007/978-94-007-0899-0_10
41. M. Ualkhanova, A.Y. Perekos, A.G. Dubovoy, D.V. Schur, Al.D. Zolotarenko, An.D. Zolotarenko, N.A. Gavrylyuk, M.T. Gabdullin, T.S. Ramazanov, N. Akhanova and S. Orazbayev, *J. Nanosci. Nanotechnol. Applications*, **3**, No. 3: 1 (2019); https://doi.org/10.18875/2577-7920.3.302
42. D.V. Schur, S.Y. Zaginaichenko, A.F. Savenko, V.A. Bogolepov, and N.S. Anikina., *Int. J. Hydrogen Energ.*, **36**, No. 1: 1143 (2011); https://doi.org/10.1016/j.ijhydene.2010.06.087
43. A.F. Savenko, V.A. Bogolepov, K.A. Meleshevich, S.Yu. Zaginaichenko, M.V. Lototsky, V.K. Pishuk, L.O. Teslenko, and V.V. Skorokhod, *NATO Security through Science Series A: Chemistry and Biology*, (Springer: Dordrecht: 2007) p. 365; https://doi.org/10.1007/978-1-4020-5514-0_47
44. D.V. Schur, S. Zaginaichenko, and T.N. Veziroglu, *Int. J. Hydrogen Energy*,**33**, No. 13: 3330 (2008); https://doi.org/10.1016/j.ijhydene.2008.03.064
45. S.Yu. Zaginaichenko, T.N. Veziroglu, M.V. Lototsky, V.A. Bogolepov, and A.F. Savenko, *Int. J. Hydrogen Energy*, **41**, No. 1: 401 (2016);

https://doi.org/10.1016/j.ijhydene.2015.08.087
46. D.V. Schur, S.Y. Zaginaichenko, and T.N. Veziroglu, *Int. J. Hydrogen Energy*, **40**, No. 6: 2742 (2015);
https://doi.org/10.1016/j.ijhydene.2014.12.092
47. Z.A. Matysina, S.Yu. Zaginaichenko, D.V. Shchur, A. Viziroglu, T.N. Viziroglu, M.T. Gabdullin, N.F. Javadov, An.D. Zolotarenko, and Al.D. Zolotarenko, *Hydrogen in Crystals* (KIM Publishing House: Kyiv: 2017).
48. D.V. Schur, S.Y. Zaginaichenko, A.F. Savenko, V.A. Bogolepov, N.S. Anikina, A.D. Zolotarenko, Z.A. Matysina, T.N. Veziroglu, and N.E. Skryabina, *NATO Science for Peace and Security Series C: Environmental Security,* (Dordrecht: Springer: 2011), p. 87;
https://doi.org/10.1007/978-94-007-0899-0_7
49. V.A. Lavrenko, I.A. Podchernyaeva, D.V. Shchur, An.D. Zolotarenko, and Al.D. Zolotarenko, *Powder Metallurgy and Metal Ceramics*, **56**: 504 (2018);
https://doi.org/10.1007/s11106-018-9922-z
50. Ol.D. Zolotarenko, M.N. Ualkhanova, E.P. Rudakova, N.Y. Akhanova, An.D. Zolotarenko, D.V. Shchur, M.T. Gabdullin, N.A. Gavrylyuk, A.D. Zolotarenko, M.V. Chymbai, I.V. Zagorulko, and O.O. Havryliuk, *Chem. Phys. Technol. Surf.*, **13**, No. 2: 209 (2022);
https://doi.org/10.15407/hftp13.02.209
51. Z.A. Matysina, Ol.D. Zolotarenko, M. Ualkhanova, O.P. Rudakova, N.Y. Akhanova, An.D. Zolotarenko, D.V. Shchur, M.T. Gabdullin, N.A. Gavrylyuk, O.D. Zolotarenko, M.V. Chymbai, and I.V. Zagorulko, *Prog. Phys. Met.*, **23**, No. 3: 528 (2022);
https://doi.org/10.15407/ufm.23.03.528
52. A.D. Zolotarenko, A.D. Zolotarenko, E.P. Rudakova, S.Y. Zaginaichenko, A.G. Dubovoy, D.V. Schur, and Y.A. Tarasenko, *Carbon Nanomaterials in Clean Energy Hydrogen Systems-II* (Dordrecht: Springer: 2011), p. 137;
https://doi.org/10.1007/978-94-007-0899-0_11
53. D.V. Schur, A.G. Dubovoy, S.Yu. Zaginaichenko, V.M. Adejev, A.V. Kotko, V.A. Bogolepov, A.F. Savenko, A.D. Zolotarenko, S.A. Firstov, and V.V. Skorokhod, *NATO Security through Science Series A: Chemistry and Biology* (Springer: Dordrecht: 2007), p. 199;
https://doi.org/10.1007/978-1-4020-5514-0_25
54. M.N. Ualkhanova, A.S. Zhakypov, R.R. Nemkayeva, M.B. Aitzhanov, B.Y. Kurbanov, N.Y. Akhanova, Y. Yerlanuly, S.A. Orazbayev, D. Shchur, A. Zolotarenko, and M.T. Gabdullin, *Energies*, **16**, No. 3: 1450 (2023);
https://doi.org/10.3390/en16031450
55. S.Y. Zaginaichenko and Z.A. Matysina, *Carbon*, **41**, No. 7: 1349 (2003);
https://doi.org/10.1016/S0008-6223(03)00059-9
56. V.A. Lavrenko, D.V. Shchur, A.D. Zolotarenko, and A.D. Zolotarenko, *Powder Metallurgy and Metal Ceramics*, **57**, No. 9: 596 (2019);
https://doi.org/10.1007/s11106-019-00021-y
57. Ol.D. Zolotarenko, E.P. Rudakova, I.V. Zagorulko, N.Y. Akhanova, An.D. Zolotarenko, D.V. Schur, M.T. Gabdullin, M. Ualkhanova, T.V. Myronenko, A.D. Zolotarenko, M.V. Chymbai, and O.E. Dubrova, *Ukr. J. Phys.*, **68**, No. 1: 57 (2023);
https://doi.org/10.15407/ujpe68.1.57
58. Ol.D. Zolotarenko, An.D. Zolotarenko, E.P. Rudakova, N.Y. Akhanova, M. Ualkhanova, D.V. Schur, M.T. Gabdullin, T.V. Myronenko, A.D. Zolotarenko, M.V. Chymbai, I.V. Zagorulko, and O.O. Havryliuk, *Chem. Phys. Technol. Surf.*, **14**, No. 2: 191 (2023);
https://doi.org/10.15407/hftp14.02.191
59. Ol.D. Zolotarenko, E.P. Rudakova, N.Y. Akhanova, An.D. Zolotarenko, D.V. Shchur,

M.T. Gabdullin, M. Ualkhanova, N.A. Gavrylyuk, M.V. Chymbai, Yu.O. Tarasenko, I.V. Zagorulko, andA. D. Zolotarenko, *Metallofiz. Noveishie Tekhnol.*, **43**, No. 10: 1417 (2021);
https://doi.org/10.15407/mfint.43.10.1417

60. Ol.D. Zolotarenko, E.P. Rudakova, N.Y. Akhanova, An.D. Zolotarenko, D.V. Shchur, M.T. Gabdullin, M. Ualkhanova, M. Sultangazina, N.A. Gavrylyuk, M.V. Chymbai, A.D. Zolotarenko, I.V. Zagorulko, and Yu.O. Tarasenko, *Metallofiz. Noveishie Tekhnol.*, **44**, No. 3: 343 (2022);
https://doi.org/10.15407/mfint.44.03.0343
61. Ol.D. Zolotarenko, E.P. Rudakova, N.Y. Akhanova, An.D. Zolotarenko, D.V. Shchur, M.T. Gabdullin, M. Ualkhanova, N.A. Gavrylyuk, M.V. Chymbai, T.V. Myronenko, I.V. Zagorulko, A.D. Zolotarenko, andO.O. Havryliuk, *Chem. Phys. Tekhnol. Sci.*, **13**, No. 4: 415 (2022);
https://doi.org/10.15407/hftp13.04.415
62. Ol.D. Zolotarenko, E.P. Rudakova, An.D. Zolotarenko, N.Y. Akhanova, M. Ualkhanova, D.V. Shchur, M.T. Gabdullin, T.V. Myronenko, A.D. Zolotarenko, M.V. Chymbai, and I.V. Zagorulko, *Metallofiz. Noveishie Tekhnol.*, **45**, No. 2: 199 (2023);
https://doi.org/10.15407/mfint.45.02.019
63. E.M. Savitsky, V.V. Baron, Yu.V. Efimov, M.I. Bychkova, and L.F. Myzenkova, *Metallovedenie Sverkhprovodyashchikh Materialov* (Moskva: Nauka: 1969), p. 265.
64. Yu.A. Izyumov and E.Z. Kurmaev, *Ukr. Phys. J.*, **2**: 193 (1974).
65. A.S. Chaves, F.C.S. Barreto, R.A. Nogueira, and B.Zĕks, *Phys. Rev. B*, **13**, No. 1: 207 (1976);
https://doi.org/10.1103/PhysRevB.13.207
66. L. Testardi, M. Weger and I. Goldberg, *Superconducting Compounds with the Structure of* β-*Tungsten* (Moskva, Mir: 1977), p. 436.
67. S.V. Vonsovsky, Yu.A. Izyumov, and E.Z. Kurmaev, *Superconductivity of Transition Metals, Their Alloys and Compounds* (Moskva: Nauka: 1977), p. 384.
68. V.I. Surikov, V.I. Pryadein, A.K. Stolts, A.P. Stepanov, A.F. Prekuya, and P.V. Geld, *Phys. Met. Metallogr.*, **34**, No. 4: 724 (1972).
69. A.I. Medvedev, A.K. Stolts, P.V. Geld, and G.N. Vorobyova, *Ordering of Atoms and Its Influence on the Properties of Alloys: Tez. Dokl. VII Vsesoyuzn. Conf.: UNC of the USSR Academy of Sciences* (Sverdlovsk: 1983), **2**: 117.
70. L.J. Vieland, A.W. Wicklund, and J.G. White, *Phys. Rev. B*, **11**, No. 9: 3311 (1975).
71. E.C. Van Reuth and R.M.Waterstrat, *Acta Crystallogr. B*, **24**: 186 (1968).
72. N.V. Ageev, N.E. Alekseevsky and V.F. Shamray, *Izvestiya AN SSSR. Metals*, **3**: 171 (1970).
73. Yu.A. Khon, V.P. Fadin, S.A. Beznosyuk and V.M. Kuznetsov, *Dokl. IV Vsesoyuzn. Confer. on the Ordering of Atoms and Its Effect on the Properties of Alloys* (Tomsk: Tomsk State University: 1974), **1**, p. 309.
74. N.V. Ageev, N.E. Alekseevsky and V.F. Shamray, *Izv. AN USSR. Metals*, **1**: 170 (1976).
75. V.S. Belovol and V.A. Finkel, *Questions of Atomic Science and Technology. Ser. Foundation and Applied Superconductivity* (Kharkiv: KhFTI of the Academy of Sciences of the Ukrainian SSR: 1977), vol. **1**, p. 6.
76. N.N. Degtyarenko, V.F. Yelesin and Yu.P. Skopintsev, *Ordering of Atoms and Its Effect on the Properties of Alloys: Tez. Dokl. VII Vsezoyuzn. Conf.,* (Sverdlovsk: UNC of the USSR Academy of Sciences: 1983), **2**, p. 42.
77. A.A. Smirnov, *Phys. Met. Metallogr.*, **58**, No. 4: 667 (1984).
78. A.A. Smirnov, *Generalized Theory of Ordering Alloys*, (Kyiv: Naukova Dumka: 1986).

79. Z.A. Matysina, D.V. Seriy, and V.A. Bondarenko, *Atomic Ordering. The Solubility of the Impurity*, *Izv. Vuzov. Physics*, **1**: 127 (1996).
80. Z.A. Matysina, S.Yu. Zaginaichenko, D.V. Schur, and V.K. Pishuk, *Proc. 11th World Hydrogen Energy Conf.* (Germany: Stuttgard: 1996) **2**: 1091.
81. Z.A. Matysina, S.Yu. Zaginaichenko, D.V. Seryi, and D.V. Schur, *Int. J. Hydrogen Energy*, **21**, Nos. 11–12: 1065 (1996).
82. W. Gorsky, *Zs. Phys.*, **50**, Nos. 1–2: 64 (1928).
83. S.Yu. Zaginaichenko, Z.A. Matysina, and M.I. Milyan, *The Solubility of Impurities in Alloys*, **2597**: 186 (1989).
84. Z.A. Matysina and M.I. Milyan, *Theory of Solubility of Impurities in Ordered Phases* (Dnipropetrovsk: Publishing House of DSU: 1991), p. 180.
85. K.H. Levchuk, T.M. Radchenko, and V.A. Tatarenko, *Metallofiz. Noveishie Tekhnol.*, **43**, No. 1: 1 (2021); https://doi.org/10.15407/mfint.43.01.0001
86. T.M. Radchenko, O.S. Gatsenko, V.V. Lizunov, and V.A. Tatarenko, *Prog. Phys. Met.*, **21**, No. 4: 580 (2020); https://doi.org/10.15407/ufm.21.04.580
87. I.M. Melnyk, T.M. Radchenko, and V.A. Tatarenko, *Metallofiz. Noveishie Tekhnol.*, **32**, No. 9: 1191 (2010).
88. V.A. Tatarenko, S.M. Bokoch, V.M. Nadutov, T.M. Radchenko, and Y.B. Park, *Defect Diffus. Forum*, **280–281**: 29 (2008); https://doi.org/10.4028/www.scientific.net/DDF.280-281.29
89. T.M. Radchenko, V.A. Tatarenko, and H. Zapolsky, *Solid State Phenom.*, **138**: 283 (2008); https://doi.org/10.4028/www.scientific.net/ssp.138.283
90. V.A. Tatarenko and C.L. Tsynman, *Solid State Ionics*, **101–103**, Pt. 2: 1061 (1997); https://doi.org/10.1016/s0167-2738(97)00376-7
91. T.M. Radchenko and V.A. Tatarenko, *Carbon Nanomaterials in Clean Energy Hydrogen Systems. NATO Science for Peace and Security Series C: Environmental Security* (Eds. B. Baranowsky, S.Y. Zaginaichenko, D.V. Schur, V.V. Skorokhod, and A. Veziroglu) (Springer Science + Business Media B.V.: 2008), p. 489; https://doi.org/10.1007/978-1-4020-8898-8_62
92. T.M. Radchenko and V.A. Tatarenko, *Hydrogen Materials Science and Chemistry of Carbon Nanomaterials. NATO Security through Science Series A: Chemistry and Biology* (Eds. T.N. Veziroglu, S.Yu. Zaginaichenko, D.V. Schur, B. Baranowski, A.P. Shpak, V.V. Skorokhod, and A. Kale) (Dordrecht: Springer: 2007), p. 229; https://doi.org/10.1007/978-1-4020-5514-0_28
93. V.A. Tatarenko and T.M. Radchenko, *Hydrogen Materials Science and Chemistry of Metal Hydrides: NATO Science Series, Series II: Mathematics, Physics and Chemistry* (Eds. T.N. Veziroglu, S.Yu. Zaginaichenko, D.V. Schur, and V.I. Trefilov) (Dordrecht, The Netherlands: Kluwer Academic Publishers:), vol. **82**, p. 123.
94. T.M. Radchenko and V.A. Tatarenko, *Int. J. Hydrogen Energy*, **36**, No. 1: 1338 (2011); https://doi.org/10.1016/j.ijhydene.2010.06.112
95. T. Radchenko, H. Zapolsky, D. Blavette, and V. Tatarenko, *Acta Cryst.*, A**60**: s71 (2004); https://doi.org/10.1107/S0108767304098599
96. S.P. Repetsky, E.G. Len, and V.V. Lizunov, *Metallofiz. Noveishie Tekhnol.*, **28**, No. 8: 989 (2006).
97. S.P. Repetsky, T.S. Len, and V.V. Lizunov, *Metallofiz. Noveishie Tekhnol.*, **28**, No. 9: 1143 (2006).

98. P. Prysyazhnyuk and D. Di Tommaso, *Mater. Adv.*, **4**, No. 17: 3822 (2023); https://doi.org/10.1039/d3ma00313b
99. P. Szroeder, I.Yu. Sagalianov, T.M. Radchenko, V.A. Tatarenko, Yu.I. Prylutskyy, and W. Strupiński, *Appl. Surf. Sci.*, **442**: 185 (2018); https://doi.org/10.1016/j.apsusc.2018.02.150
100. S.M. Bokoch, M.P. Kulish, T.M. Radchenko, and V.A. Tatarenko, *Metallofiz. Noveishie Tekhnol.*, **26**, No. 3: 387 (2004).
101. S.M. Bokoch, M.P. Kulish, V.A. Tatarenko, and T.M. Radchenko, *Metallofiz. Noveishie Tekhnol.*, **26**, No. 4: 541 (2004).
102. A.G. Solomenko, R.M. Balabai, T.M. Radchenko, and V.A. Tatarenko, *Prog. Phys. Met.*, **23**, No. 2: 147 (2022); https://doi.org/10.15407/ufm.23.02.147
103. T.M. Radchenko, *Metallofiz. Noveishie Tekhnol.*, **30**, Spec. Iss.: 195 (2008); *Metal Physics and Advanced Technologies*, **19**, No. 2: 211 (2001).
104. D.S. Leonov, T.M. Radchenko, V.A. Tatarenko, and Yu.A. Kunitsky, *Defect Diffus. Forum*, **273–276**: 520 (2008); https://doi.org/10.4028/www.scientific.net/DDF.273-276.520
105. K. Cornell, H. Wipf, U. Stuhr, and A.V. Skripov, *Solid State Communications*, **101**, No. 8: 569 (1997); https://doi.org/10.1016/S0038-1098(96)00653-9
106. F. Mebtouche, T. Zergoug, S.E.H. Abaidia, J. Bertsch, A. Seddik Kebaili, and A. Nedjar, *Comput. Theor. Chem.*, **1178**, No. 15: 112781 (2020); https://doi.org/10.1016/j.comptc.2020.112781
107. Chunlei Shen, Yunping Jia, Canhui Xu, Shuanglin Hu, Xiaosong Zhou, and Xinggui Long, *Surface Science*, **725**: 122149 (2022); https://doi.org/10.1016/j.susc.2022.122149
108. Q. Liu, Z. Zhang, S. Liu, and H. Yang, *Adv. Eng. Mater.*, **20**, No. 5: 1700679 (2018); https://doi.org/10.1002/adem.201700679
109. J. Wang and H. Gong, *Int. J. Hydrog. Energy*, **39**, No. 11: 6068 (2014); https://doi.org/10.1016/j.ijhydene.2014.01.126
110. M. Schlereth and H. Wipf, *J. Phys.: Cond. Matt.*, **2**, No. 33: 6929; https://doi.org/10.1088/0953-8984/2/33/005
111. L. Chen, Q. Wang, W. Jiang, and H. Gong, *Metals*, **9**, No. 2: 121 (2019); https://doi.org/10.3390/met9020121
112. S. Zhu, R.J. Zhang, L. Wan, Y.K. Guo, R.Y. Zhou, and T. Gao, *Mater. Chem. Phys.*, **277**: 125549 (2022); https://doi.org/10.1016/j.matchemphys.2021.125549
113. Y.J. Choi, J.W. Choi, H.Y. Sohn, T. Ryu, K.S. Hwang, and Z.Z. Fang, *Int. J. Hydrog. Energy*, **34**, No. 18: 7700 (2009); https://doi.org/10.1016/j.ijhydene.2009.07.033
114. M. Calizzi, D. Chericoni, L.H. Jepsen, T.R. Jensen, and L. Pasquini, *Int. J. Hydrog. Energy*, **41**, No. 32: 14447 (2016); https://doi.org/10.1016/j.ijhydene.2016.03.071
115. F. Yan, I. Mouton, L.T. Stephenson, A.J. Breen, Y. Chang, D. Ponge, D. Raabe, and B. Gault, *Scr. Mater.*, **162**: 321 (2019); https://doi.org/10.1016/j.scriptamat.2018.11.040
116. M. Pozzo and D. Alfè, *Int. J. Hydrog. Energy*, **34**, No. 4: 1922 (2009); https://doi.org/10.1016/j.ijhydene.2008.11.109
117. M.W. Davids, M. Lototskyy, A. Nechaev, Q. Naidoo, M. Williams, and Y. Klochko, *Int. J. Hydrog. Energy*, **36**, No. 16: 9743 (2011); https://doi.org/10.1016/j.ijhydene.2011.05.036

118. V.N. Bugayev, V.G. Gavrilyuk, V.M. Nadutov, and V.A. Tatarenko, *Fizika Metallov i Metallovedenie*, **68**, No. 5: 931 (1989).

Received 28.09.2023;
in final version, 17.11.2023

Ан.Д. Золотаренко[1,2], Ол.Д. Золотаренко[1,2], З.А. Матисіна[1], Н.А. Швачко[1,3], Н.Є. Аханова[4,5], М. Уалханова[5], Д.В. Щур[1,6], М.Т. Габдуллін[4], М.Т. Картель[2], Ю.М. Солонін[1], Ю.І. Жирко[6], Д.В. Ісмаїлов[5,7], О.Д. Золотаренко[1], І.В. Загорулько[8]

[1]Інститут проблем матеріалознавства ім. І.М. Францевича НАН України,
вул. Омеляна Пріцака, 3, 03142 Київ, Україна
[2]Інститут хімії поверхні ім. О.О. Чуйка НАН України,
вул. Генерала Наумова, 17, 03164 Київ, Україна
[3]Київський національний університет будівництва і архітектури,
просп. Повітрофлотський, 31, 03037 Київ, Україна
[4]Казахстансько-британський технічний університет,
вул. Толе бі, 59, 050040 Алмати, Казахстан
[5]Казахський національний університет ім. Аль-Фарабі,
просп. Аль-Фарабі, 71, 050040 Алмати, Казахстан
[6]Інститут прикладної фізики НАН України,
вул. Петропавлівська, 58, 40000 Суми, Україна
[7]НАТ «Казахський національний дослідницький технічний університет
імені К.І. Сатбаєва»,
вул. Сатбаєва, 22, 050013 Алмати, Казахстан
[8]Інститут металофізики ім. Г.В. Курдюмова НАН України,
бульв. Академіка Вернадського, 36, 03142 Київ, Україна

ГІДРОҐЕН У СПОЛУКАХ І СТОПАХ ІЗ СТРУКТУРОЮ *A*15

У даній роботі виконано теоретичне дослідження атомового впорядкування у стопі A_3BC_x. Вивчено взаємний вплив упорядкування та розчинности домішки *C* у стопі A_3B. Знайдено та досліджено залежності розчинности від складу стопу, температури, ступеня далекого порядку. Також одержано критерії прояву екстремальности у концентраційній і температурній залежностях розчинности. Атомове впорядкування вивчено за допомогою методу середніх енергій; особливості розчинности домішки *C* у стопі A_3B вдалося з'ясувати за допомогою конфіґураційного методу. Експерименти, що підтверджують результати теорії, наразі невідомі авторам. Одначе наявні експериментальні дані щодо визначення температур мартенситного перетворення (T_m) і переходу у надпровідний стан (T_c) для стопу Nb_3SnH_x дають змогу сподіватися та стверджувати стосовно можливої відповідности даних теорії й експерименту.

Ключові слова: кристалічна структура, структура типу *A*15, стопи, сполуки, металогідриди, водень, фазові перетворення, переходи лад–безлад, розчинність.